Ranking multiple infiltration formulas to determine their match to trustable hydrogeological parameters obtained under highly controlled conditions. Santiuste basin, Los Arenales Living Lab, Spain

Classificazione di molteplici formule di infiltrazione per determinarne la corrispondenza con parametri idrogeologici affidabili ottenuti in condizioni fortemente controllate. Bacino di Santiuste, Los Arenales Living Lab, Spagna

Enrique FERNÁNDEZ ESCALANTE[a,b] ✉ , Noelia CRESPO ARRIBAS[c], Sergio FERNÁNDEZ CORDERO [d]

[a] Tragsa I+D+i, Maldonado 58, Madrid 28006, Spain - email ✉ : *efernan6@tragsa.es*
[b] Universidad Politécnica de Madrid, Av. Puerta de Hierro 2-4, Madrid 28040, Spain
[c] Tragsa Canarias, Calle Ibaute 27 Alto, Santa Cruz de Tenerife, 38111, Spain. - email: *ncrespo1@tragsa.es*
[d] ICAI, ETS Ingeniería, Alberto Aguilera, 23, Madrid 28015 Madrid, Spain - email: *202305407@alu.comillas.edu*

Abstract

Hydraulic conductivity is a crucial variable in hydrological studies involving groundwater resources. It provides insight into underground water flow and is essential for creating numerical groundwater models, evaluating an aquifer's potential for water supply and intentional recharge, and determining site suitability for construction projects. Many surveys and tests can be used to estimate hydraulic conductivity. Authors have developed a methodology to determine the best method for estimating hydraulic conductivity in a intensely monitored area. This involves comparing parameters observed on-site and applying widely-accepted formulas from hydrogeological literature. The methodology was implemented in the Santiuste basin, which is part of the Los Arenales Managed Aquifer Recharge (MAR) systems. In this area, reliable hydrological data sets have been collected for approximately 15 years using various sensors under highly controlled conditions. Direct measures of real horizontal (K_{xy}) and vertical (K_z) hydraulic conductivities, along with other parameters, have been assessed to be compared with the results of formulas.

The authors have tested a total of 20 formulas and methods to evaluate which theoretical formula best matches the hydraulic conductivities obtained in the field. We have proposed a ranking of formulations based on their accuracy in relation to the observed data. We have also developed a correlation matrix among the different environmental conditions and MAR water flow to assess the relationship among several parameters, and the weight of each for groundwater movement in this specific MAR system. The methodology presented can help to determine the best groundwater flow interpretation formulas in particular conditions.

Riassunto

La conducibilità idraulica è una variabile fondamentale negli studi idrologici che riguardano le risorse idriche sotterranee. Essa fornisce informazioni sul flusso idrico sotterraneo ed è essenziale per la creazione di modelli numerici di circolazione delle acque sotterranee, per la valutazione del potenziale di un acquifero per l'approvvigionamento idrico e la ricarica artificiale, e per la determinazione dell'idoneità di un sito per progetti di costruzione. Molte indagini e prove possono essere utilizzate per stimare la conducibilità idraulica. Gli autori hanno sviluppato una metodologia per determinare il metodo migliore per stimare la conducibilità idraulica in un'area intensamente monitorata. Ciò ha comportato il confronto dei parametri osservati in sito e l'applicazione di formule ampiamente usate nella letteratura idrogeologica. La metodologia è stata implementata nel bacino di Santiuste, che fa parte dei sistemi di Managed Aquifer Recharge (MAR) di Los Arenales. In quest'area, set di dati idrologici affidabili sono stati raccolti per circa 15 anni utilizzando vari sensori in condizioni fortemente controllate. Misure dirette della conducibilità idrauliche orizzontale (K_{xy}) e verticale (K_z) reali, insieme ad altri parametri, sono state valutate per essere confrontate con i risultati ottenuti dalle formule.

Gli autori hanno testato un totale di 20 formule e metodi per valutare attraverso quale formula teorica si ottengano risultati maggiormente corrispondenti alle conducibilità idrauliche ottenute sul campo. Abbiamo proposto una classificazione delle formule basata sulla loro accuratezza in relazione ai dati osservati. Abbiamo anche sviluppato una matrice di correlazione tra le diverse condizioni ambientali e il flusso idrico MAR per valutare la relazione tra diversi parametri e il peso di ciascuno per il movimento delle acque sotterranee in questo specifico sistema MAR. La metodologia presentata può aiutare a determinare le migliori formule di interpretazione del flusso delle acque sotterranee in condizioni particolari.

Introduction

Aquifers can be recharged by anthropic activity, either in an intentional form, by, e.g., managed aquifer recharge (MAR) (DINA-MAR, 2010), or unintended, such as transverse structures in river courses, leakages from pipes, etc. (CIS, 2023).

Accurate parameters are necessary to design appropriate managed aquifer recharge (MAR) schemes, especially regarding the suitable inflow to be directed in an infiltration pond, or the reasonable dimension of MAR channels to infiltrate the available volume of water to store in the subsurface (Guyennon et al., 2017).

The determination of precise hydraulic conductivities (K_{xyz}), and the storage coefficient (S), are key to design and dimension efficient MAR systems, but their determination is not always exact (Dillon et al., 2019), and usually measuring methods and interpretations for groundwater flow differ (Bouwer, 2002). Several methods are used in the countryside, e.g. infiltrations test, slug test, pumping test, etc., but the results, depending on the selected methodology, vary even above two orders of magnitude (Custodio, 1986; Bouwer, 1999; Fernández et al., 2009). An effective project requires an accurate knowledge of the aquifer and groundwater system and behaviour, quantified through necessary parameters. Permeability is an intrinsic variable of each material, as well as hydraulic conductivity, concept more dependent on fluid properties, especially viscosity. For water, both parameters are practically identical, but not for high density fluids, e.g. oil, with a much higher variation. Therefore, authors will refer to hydraulic conductivity as groundwater flow velocity in MAR systems through the unsaturated and saturated means, affected by environmental conditions.

Los Arenales MAR systems (Castile and Leon, Spain), which constitute a Living Lab, has various stations gathering data of the unsaturated zone, known as ZNS stations (Fernández & Merino, 2009). These stations have several sensors to monitor humidity (after, soil water content), temperature, conductivity, and capillary tension in the vadose zone, as well as water table evolution, temperature and conductivity of the groundwater in the saturated zone, collecting data every 15 minutes from 2009 until now. The construction of piezometers and the presence of wells near these stations allow for calculating reliable groundwater flow parameters from direct observation and indirect calculation, as well as determining the humidification bulb morphology during MAR recharge cycles and, therefore, the anisotropy of the receiving medium. Other parameters, such as the capillary tension, caused by the air trapped in the recharge system, are monitored too to assess gas clogging. (Fernández & Senent, 2011). ZNS-1 station is placed at scarce meters from the infiltration pond and west channel constructed in the heading of the Santiuste basin's MAR system (see Figure 4). Sensors, wells and piezometers are providing data to adjust the length of the MAR canals used to increase underground water resources for irrigation in this site (Tragsa, 2015).

Generally speaking, the most efficient MAR system is one with a maximum infiltration rate and minimum clogging accumulation (Lippera et al., 2023). The determination of the most accurate formulas for future recharge studies in equivalent MAR areas is the main target and it is an asset too.

Objectives

The main purpose of this article is to check different infiltration formulas to select the most appropriate in future studies. It also aims to determine the most accurate hydraulic parameters using direct in-field measurements for validation. Both achievements require the characterization of the aquifer and the study of groundwater flow in Santiuste basin, one of the Los Arenales MAR systems.

The hydrodynamic monitoring of the saturated and unsaturated zones of the aquifer aims to meet the following objectives:

1. To quantify the infiltration rates (H and V) of the artificial recharge water after the measurements taken during 12 artificial recharge cycles between 2008 and 2022. Notice the operation began in 2002.
2. To better understand the asymmetry of the humidification bulb beneath the infiltration pond and the artificial recharge channels departing from both down stream's corners, based on the anisotropy of the system.
3. To determine the necessary data and parameters to be collected in the field to apply up to 20 equations to estimate hydraulic conductivities, to be compared to direct measurements.
4. To study the validity of various equations for the type of aquifer under study (high permeability fine-grained granular), and the accuracy of the results with respect to those obtained in the field (under different environmental conditions and intensively monitored), establishing an equations ranking.
5. To advance the study of the correlation among hydraulic conductivity, soil moisture, soil temperature, water table depth, capillary tension, and precipitation in the previous days whilst the unsaturated zone is saturated by the humidification bulb.

Materials and Methods
Background

Description of the living lab

Santiuste Basin has an area about 42 km^2, and is allocated in the West of Segovia and SE of Valladolid provinces. It lies among the municipalities of Llano de Olmedo, Villeguillo, Coca and Santiuste de San Juan Bautista, on the left bank of the Voltoya and Eresma Rivers. The aquifer is characterised by a Quaternary sandy formation, up to 55 metres thick (Arévalo Unit), which fills a complex cavity of a Tertiary clayey (Cuestas Facies), or sandy-clayey (Puente Runel Facies) substrate (IGME, 1982). The detailed geology, description of the aquifer's facies and hydrogeological behaviour are described in detail in the references Fernández, 2005, 2010 & 2014.

The artificial recharge system consists of infiltration canals, ponds and wells, which recharge excess river water during winter for irrigation in the summer. It starts at a small

reservoir on the Voltoya River. From there, a 9,864-metre-long underground pipe runs downhill to a 36 m³ reservoir (heading of the MAR system), housing a flowmeter. This is followed by a 14,322 m² stagnation and infiltration basin, from which two main MAR channels extend. The first channel, called "Caz Viejo" (or East channel), began operating in 2002; and the "Caz Nuevo" (or West channel), started operating in 2005 (Fig. 1) (MAPA, 2005; MAPAMA, 2008; Fernández, 2014).

The East channel has 54 stopping devices to increase infiltration over its surface area (about 33,300 m²), accounting for infiltration through the bottom and the sides (MARSOL, 2016a).

The West channel has a total length of 17,293 m. It is located in the sector of maximum thickness of the aquifer resulting in a large effective surface for recharge (nearly 100%).

Figure 1 illustrates the Managed aquifer recharge device on an isopach map of the Quaternary sandy aquifer, displaying its various construction elements and position in Spain.

The mean flow from the Voltoya River is approximately 0.5 m³/s, with a MAR allowance period extending from November 1st to April 30th, but this allowance may change depending on the amount of precipitation in the hydrological year. According to the restrictions, if the flow rate at the Voltoya River gauging station in Coca village drops below 1,0 m³/s, the water recharge process must be stopped immediately (PHD, 2016). The construction of the project was initially carried out by the Spanish Ministry of Agriculture and the regional government, Junta de Castilla y León (JCL) (IRYDA, 1991, IGME, 2000 & IMTA, 2017).
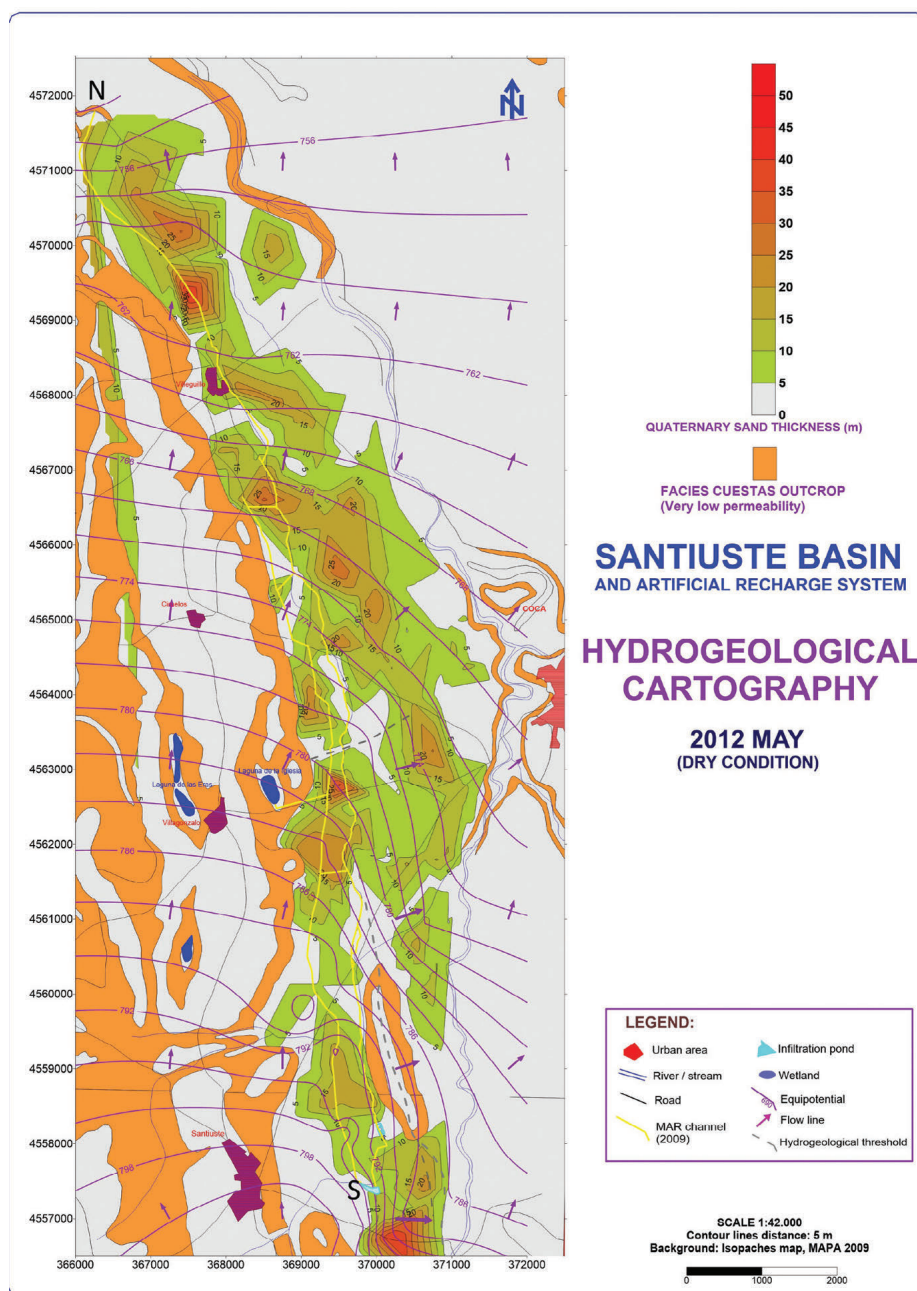

Fig. 1 - Santiuste basin´s MAR system depicted above an iso-thicknesses Quaternary aeolian sand cartography. Modified from MARSOL, 2016b.

Fig. 1 - Il sistema MAR del bacino di Santiuste rappresentato su una carta delle curve di iso-spessore delle sabbie eoliche Quaternarie. Modificato da MARSOL, 2016b.

The MAR system in Santiuste has been continuously operating since 2002, infiltrating volumes of 2.60 Mm³/year as an average, with the range varying between zero (in hydrological years 2011/12 and 2018/19), and 5.11 Mm³ (in 2005/06) (Fig. 2). Removing the dry hydrological years without recharge, the mean is 2.86 Mm³ / MAR cycle. From December 2002 to June 2024, there have been a total of 1,954 days of MAR, resulting in a total infiltrated volume of 57.30 Mm³ inserted intentionally in the whole Santiuste Integrated Water Resources Management (IWRM) system. The average flow rate in the MAR channels has been 403.98 L/s during the recharge days. This natural system assures the character of nature-based solution associated to this MAR systems (López-Gunn, 2021; López-Gunn et al., 2021), and monitoring plans application (Gómez-Espín, 2019; ITACYL, 2020).

The hydraulic parameters for this specific area vary across different sources due to variations in data collection methods and interpretation (IRYDA, 1991; MAPA, 1999; IGME, 2000, Fernández, 2005; MAPA, 2005; Fernández et al., 2009). Most technical references do not separate the permeability components into horizontal and vertical.

Although the Santiuste basin area has been considered isotropic and homogeneous in theory, in practice there are differences between horizontal and vertical permeabilities, especially in sectors with interspersed clay levels and minerals (Sanz Montero et al., 2013).

Additionally, there is a slight difference in the main components of horizontal hydraulic conductivity (i.e., K_x and K_y). Pumping tests to date have provided the most reliable hydraulic conductivity data, yielding values corresponding to the average of the aquifer (MAPA, 2005 & 2009).

In MAPA (1999; 2005), for the small sector studied, K_v was estimated at 2.29 - 4.70 m/day, with a storage coefficient (S) of 14.12. Lefranc tests gave a horizontal hydraulic conductivity (K_h) of 3.14 m/day and a vertical hydraulic conductivity (K_v) of 1.54. Newer pumping tests yielded a storage coefficient (S) ranging between 18 and 21 (MAPA, 2005 & 2009).

Other authors have reported values of K_h of 15 m/day, and 0.5 of K_v, calculated from the hydraulic gradient of 1 to 6% (MOPTMA, 1994; MIMAM, 2002), permeability of 4 to 5 m/day in the ZNS-1 sector, transmissivities of 1,200 - 1,400 m²/day, based from the data collected during the first artificial recharge cycle (Fernández and Merino, 2009; Fernández & San Sebastián, 2017), and considering the direct influence of clogging on groundwater flow reduction (Fernández & San Sebastián, 2019). Therefore, the permeability in the area is medium or high, according to the scale of Terzaghi & Peck (Terzaghi & Peck, 1967).

Infiltration formulas. State-of-the-art
Formulas and equations for the interpretation of infiltration tests

The hydraulic conductivity of a medium is an average representation of the values of horizontal, vertical, unsaturated, partially saturated and saturated zone permeabilities (MARSoluT, 2021).

There are different methodologies to determine average values of hydraulic conductivity, as opposed to tests in isolated sections of boreholes, on the surface, or laboratory tests (which are not part of this study). In general, four groups of tests have been established by the authors (Table 1, third column):

1. Infiltration test using an excavated ditch: This test involves creating a drawdown-time log from an excavation of known dimensions, while maintaining a constant (1a) or variable (1b) water level.
2. Infiltration test using a borehole or well: This test involves producing a drawdown-time log from a borehole or well of known dimensions, which can be open (2a) or closed (2b).
3. Slug tests: This test includes filling the excavation or borehole almost instantly and recording the decrease in the water level over time. The obtained permeability will mainly be vertical, and will be determined under semi-saturated or unsaturated conditions (dry environment with natural field capacity).
4. Pumping tests: These tests are conducted in wells or boreholes, ideally with an observation piezometer within the radius of influence.

The formulas and tests, which are to be compared with field measurements, are provided in Table 1. The table includes some common equations from the literature on artificial recharge of aquifers, but it is not exhaustive.

MAR volumes diverted from Voltoya river. Santiuste Basin (Mm³ / h. year)
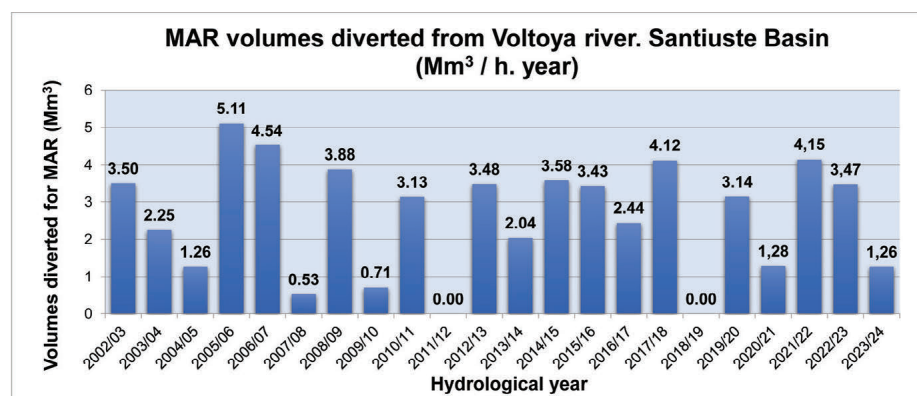
Fig. 2 - Managed Aquifer Recharge (MAR) volumes in Santiuste basin per hydrological year (from October to September). Activity between 2002 and 2024. Annual mean: 2.60 Mm³ per year and 2.86 per MAR cycle. Updated from Fernández and López, 2021.

Fig. 2 - Volumi di Managed Aquifer Recharge (MAR) nel bacino di Santiuste per un anno idrologico (da Ottobre a Settembre). Attività tra il 2002 e il 2024. Media annuale: 2.60 Mm³ per anno e 2.86 per ciclo di MAR. Aggiornato da Fernández e López, 2021.

Tab. 1 - Methods and equations used to calculate hydraulic conductivities from in-field data classified by type of test and in alphabetical order for each class (1 to 4). Not comprehensive.

Tab. 1 - Metodi ed equazioni usate per calcolare le conducibilità idrauliche da dati di campo classificati per tipologia di test e in ordine alfabetico per ciascuna classe (da 1 a 4). Non esaustiva.

Method	Equation	Theoretical type of essay / source
Gilg-Gavard (constant level)	$K = \dfrac{Q}{600 \cdot A \cdot h_m}$	Infiltration test (1a) (Custodio & Llamas, 1983)
Gilg-Gavard (variable level)	$K = \dfrac{1{,}308 d^2}{A \cdot h_m} \cdot \dfrac{\Delta h}{\Delta t}$	Infiltration test (1b) (Custodio & Llamas, 1983)
Double ring test	ASTM D3385-18	Infiltration test (1 a-b) (ASTM, 2018)
Darcy	$K = Q / A \cdot I$	Infiltration test (1b) (Darcy, 1856)
Ernst	$h = s \dfrac{D_v}{K_l} + \dfrac{sL^2}{8KD} + sLW_r$	Infiltration test (1b) (Ernst, 1950)
Green & Ampt	$f = -K_s \dfrac{dh}{dz}\ \dfrac{dh}{dz} = $ hydraulic gradient $\left[\text{cm}^3\text{s}^{-1}\text{cm}^{-2} \right]$ $f = -K_s \dfrac{h_f - h_o}{Z_f} \left[\text{cm}^3\text{s}^{-1}\text{cm}^{-2} \right]$	Infiltration test (1b) (Green & Ampt, 1911)
Kostiakov	$T = L / b \cdot m$	Infiltration test (1b) (Kostiakov, 1932)
Kraijenhoff van de Leur	$h' = \dfrac{\pi}{2\mu\alpha} s_0 e^{-ct}$ $\qquad$ $\alpha = \dfrac{\pi KD}{\mu L_0^2}$	Infiltration test (1b) (Kraijenhoff van de Leur, 1958)
Lewis	$l = kt^n$	Infiltration test (1b) (Lewis, 1937)
Matsuo-Akai	$K = \dfrac{-C}{60 \cdot t} \cdot \ln\left(\dfrac{h+C}{H_0+C} \right)$ $\qquad$ $C = \dfrac{L \cdot l}{2 \cdot (L+l)}$	Infiltration test (1b) (Matsuo-Akai, 1952)
Lefranc (ISO, 2012) (with FF)	$K = \dfrac{Q}{C \cdot h}$ $\qquad$ $C = \dfrac{2\pi L}{\ln(L/d) + \sqrt{(L/d)^2 + 1}}$	Infiltration test. Open circuit (2a) (UNE, 2012)
Lefranc (ISO, 2012) (without FF, variable load)	$k = \dfrac{(de)^2 \ln\left(\frac{2h}{d}\right)}{8ht} \cdot \ln\dfrac{H_1}{H_2}$	Infiltration test. Open (2a) (ISO, 2012)
Cooper, Bredehoeft & Papadapulos (1967)	$\dfrac{h_t}{H_0} = F(\alpha,\beta)$ $\quad$ $F(\alpha,\beta) = \dfrac{8\alpha}{(\pi)^2} \int_0^\infty e^{\left(\frac{-\beta u^2}{\alpha}\right)} \dfrac{1}{u^2 \Delta u} du$ $a = \dfrac{R_w^2 S}{R_c^2}$ $\qquad$ $\beta = \dfrac{Tt}{R_c^2}$	Slug test (3) (Cooper et al., 1967)
Bouwer & Rice (1976)	$F = \dfrac{2\pi L_t}{\ln\left[\frac{R_t}{R_w}\right]}$ $\dfrac{h_t}{H_0} = \exp\dfrac{-kt}{\pi R_c^2} F$	Slug test (3) (Bouwer & Rice, 1976; Bouwer, 1989)
Hvorslev (1951)	$\dfrac{h_t}{H_0} = \exp\left(\dfrac{-kt}{\pi R_c^2} F \right)$	Slug test (3) (Hvorslev, 1951)
Hantush (1959)	$s = \dfrac{Q}{2\pi T} \ln\left(\dfrac{1{,}12 \cdot B}{r} \right)$ $\qquad$ $B = \sqrt{\dfrac{Tb'}{K'}}$	Pumping tests (4) (Hantush, 1959)
Jacob (1946)	$s = 0{,}183 \dfrac{Q}{T} \log \dfrac{2{,}25 \cdot T \cdot t}{r^2 \cdot S}$	Pumping tests (4) (Cooper & Jacob, 1946)
Newman (1975)	$s = \dfrac{Q}{4\pi T} W(u_s, u_s, \beta)$ $\quad$ $\beta = \dfrac{r^2 K_z}{b^2 K}$; $u_A = \dfrac{r^2 S}{4/T}$; $u_s = \dfrac{r^2 S_r}{4/T}$	Pumping tests (4) (Newman, 1975)
Theis (1935)	$s = \dfrac{Q}{4\pi T} W(u)$ $\quad$ $u = \dfrac{r^2 S}{4Tt}$	Pumping tests (4) (Theis, 1935)
Thiem (1906)	$s_1 - s_2 = \dfrac{Q}{2\pi T} \ln \dfrac{r_2}{r_1}$	Pumping tests (4) (Thiem, 1906)

The data have been interpreted using the methodologies set out above. A detailed explanation of each, including the terms for each equation, is extended in Annex 1.

Scientific State-of-the-Art

ANNEX 1 extends the information exposed in table 1, and data gathering (divided into automatic and manual data collection).

Materials
Automatic data collection

At the beginning of 2008, the ZNS-1 station (Figure 3a) was established to study and monitor the changes in humidity, temperature and capillary tension in the unsaturated subsoil zone in the vicinity of the West channel for the artificial recharge of the Santiuste basin aquifer (Tragsa, 2008; Fernández et al., 2009).

The station consists of three sensors; initially two SDEC HMS 9000 humidity-thermometers that also measure dielectric permittivity. These sensors were replaced by TRIME PICO 64, from IMKO (IMKO, 2016) on 28/11/2016 (Figure 3b). The new sensors measure humidity percentage, temperature, and electrical conductivity. The upper sensor was initially located at a depth of 0.5 m, but was later deepened to 1.05 m in October 2014, the same depth as the tensiometer. The lower sensor was permanently placed at a depth of 2.10 m, to ensure saturation during most artificial recharge cycles (Fernández & Senent, 2011).

Since 2016, groundwater's level, electrical conductivity and temperature were included in the measurements by means of a CTD Hydrus 21 sensors (IMKO, 2016) installed in a nearby piezometer (Fig. 3c).

The capillary tension (in cbar) is monitored thank to a tensiometer Bourdon-type SDEC Mod. SR1000 sensor (Fig. 3d), placed between the two humidimeter-thermometers (SDEC, 2006). Its porous ceramic cup is located at about 1.05

m depth, i.e. about 75 cm above the highest water level in the West MAR channel in most of the artificial recharge cycles. These sensors were calibrated and verified in situ by Microterm 4800 (Fig. 3e) (SDEC, 2008).

Five parameters are continuously monitored, including two humidity measurements, two temperature measurements and one capillary tension measurement. Data are collected every 15 minutes and recorded using a Campbell 8000 data logger (Fig. 3f). Additionally, instruments for remote data collection were installed (MARSOL, 2016a-b).

Piezometer 1 (Fig. 4) was constructed 18.30 m from station ZNS-1, and it was equipped with a Decagon Hydros 21 sensor (Fig. 3c) that measures water level, conductivity and temperature (METER, 2016). The sensors were located at 2.10 m depth, at the same altitude as the TRIME PICO 64, and 30 cm lower than the mean level of the water in the West channel (dam-regulated).

Meteorological data are obtained from the Inforiego SG-02 station in Nava de la Asunción, belonging to the Inforiego Network of the Junta de Castilla y León, located at 6,747 m from station ZNS-01. Its position is UTM: X: 376254.97 / Y: 4559087.71 / Z: 822 mamsl). This fully-equipped station provides data that can be accessed in quasi-real time on the internet via inforiego.org (see references).

In-person data gathering

The necessary data to be able to apply the 20 formulas selected for infiltration and pumping tests required the following instrumentation:
- Rotating probe with continuous core recovery.
- Impulsion pumps to inject water with a determined flow rate (one for maximum flow rates of 65 L/minute, and another one for up to 1,000 L/minute).
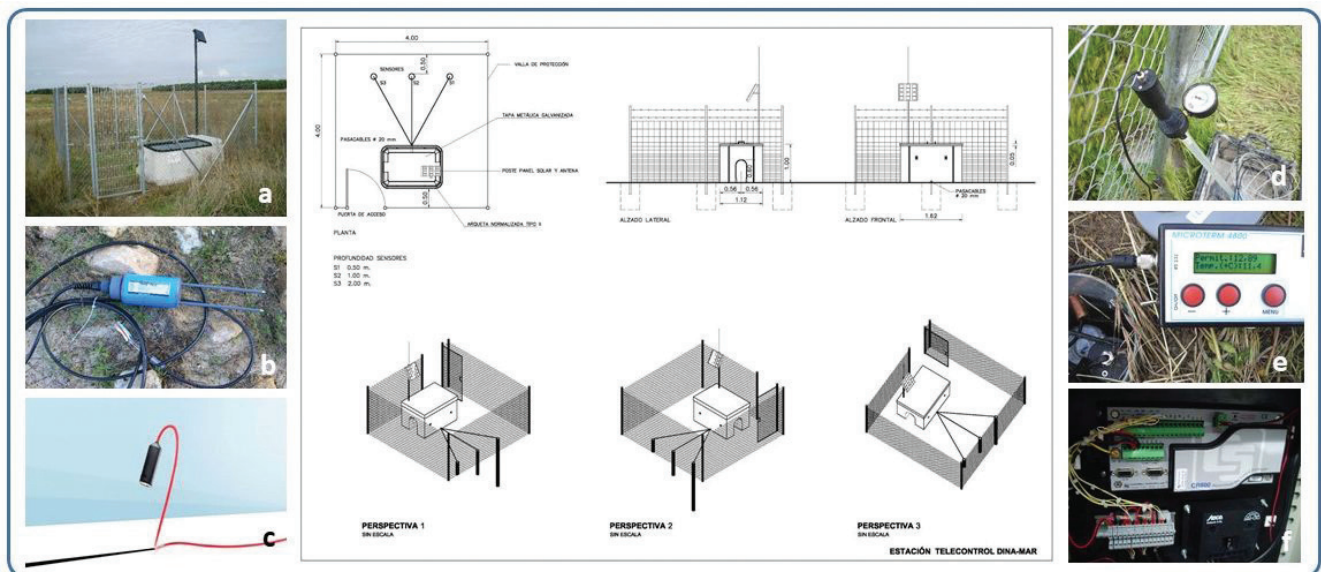

Fig. 3 - ZNS-1 station´s arrangement of installed instrumentation. Appearance of ZNS-1 (a), Humidity-thermometers (b), CTD Hydros 21 sensor (c), Bourdon tensiometer (d), Microterm for in situ verification of the data taken by the first sensor (e), and data logger to store the information (f) (modified from the original works project, Tragsa, 2008).

Fig. 3 - Configurazione della strumentazione installata nella stazione ZNS-1. Immagine della ZNS-1 (a); Termo-idrometri (b); sensori CTD Hydros 21 (c); tensiometro Burdon (d); Controllo in situ del primo sensore (e), e data logger per salvataggio delle informazioni (f) (modificato dai lavori originali del progetto, Tragsa, 2008).

- Meter with gate-type shut-off valve.
- Totalising flow meter for reduced flow rates with an accuracy of 10-4 m^3.
- Water tank with a capacity of 12 m^3 for instantaneous filling of the well or piezometer in slug tests.
- 50 m water level probe with acoustic and light indicator.

Additional elements:

- Hoses for slug tests, both pneumatic and hydraulic, of sufficient length and diameter.
- CTD sensors for accurate the water level (1 mm) measurements. These replace the water level tape and stopwatch.
- Data logger to store captured data from the sensors.
- Precise safety equipment for operators and technicians, including PPE.

IT technologies applied

The application of IT technologies has been conducted with Multicorrelation_PRyES_v1.7. It is a script programmed in Phyton from ICAI (Comillas Pontifical University, 2024). This software enables multivariable analysis of diverse data through descriptive statistics to generate a visually intuitive correlation matrix. This matrix illustrates how various variables interrelate, facilitating clear interpretation and understanding.

Methods
Configuration of the automatic data capture system

The study of water level variation in the vicinity of the infiltration pond and the artificial recharge West channel has been conducted mainly using data from the ZNS-1 station, piezometer 1, wells 47B and 48; slug tests in the STR and STC piezometers inside the headwater reservoir (Fig. 4 and Table 2). Additionally, results from double ring infiltration tests were considered. Furthermore, a pumping test was conducted in well 47B in October 2008, and measurements were taken on the arrival of the humidification bulb from the infiltration basin to both wells at the beginning of three recharge cycles: 2008/09 (Fernández & García, 2009), 2014/15 (MARSOL, 2016a), and 2017/18 (Fernández et al, MARSOLUT, 2021, 2023b) (see "results" section).

Methods for k_x calculation
Arrival of the humidification bulb at wells 47b and 48

The well 47B, according to MAPA 2009's code, is 65.6 m from the closet margin of the infiltration pond downstream of the hydraulic gradient (Fig. 4), with an "approximate" north-south orientation (the source area of the sediment comes from the east, and it is also the direction of the groundwater flow lines (S>N). Thus, the permeability is comparable to the horizontal component (K_x).

The well 48 (MAPA 2005's code, modified to well 42 in MAPAMA, 2008) has an elevation of 801.49 meters above mean sea level (mamsl) for mean ground level, and is located 78.8 metres upstream of the hydraulic gradient (Fig. 4). The line between the well and the infiltration pond is

approximately north-south. Thus, the horizontal permeability obtained is considered comparable to the K_x.

An observation of the water table variation in wells 47b and 48 (Fig. 4) has been conducted since the beginning of the filling of the infiltration pond with river water in the MAR cycles 2008/09, 2014/15, and 2017/18. It takes an average of 5 days to fill the infiltration pond. During this time, the humidification bulb is generated and enters into "vertical control" (it reaches the water table), and simultaneously, it begins to move horizontally in a radial manner, from the margin of the infiltration basin. During its bulb's advance, the phreatic level rises slightly as it moves with a mostly horizontal component. When the bulb reaches wells 47b and 48 (both of which penetrate the impermeable base of the shallow Aeolian aquifer under study), it directly influences the variation of the water table. This has allowed accurate determination of up to three K_x values (results section).

Pumping test

The pumping test of well 47b, using two adjacent wells (A and B) as piezometers (Fig. 4), was conducted in October 2008, before the 2008/09 artificial recharge cycle. This cycle was intensely monitored (Fernández, 2014) ("Results" section).

Methods for K_y calculation
Observed horizontal permeability between the artificial recharge channel, piezometer 1, and the zns-1's deepest sensor

The sensors are positioned transversally to the West channel, with one upstream and one downstream of the hydraulic gradient. They are used to detect and quantify the
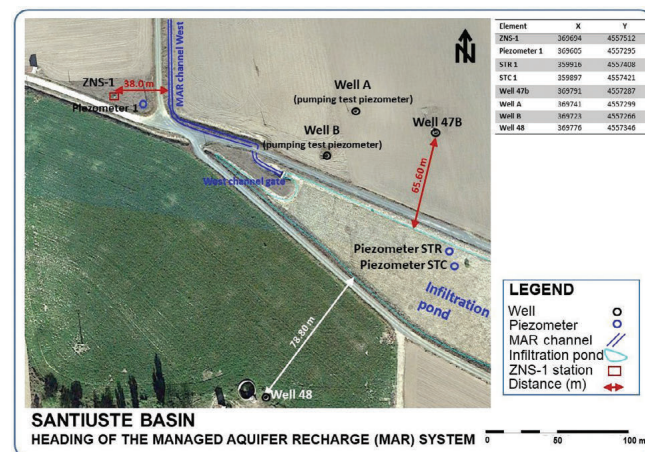

Fig. 4 - Scheme of the key elements available to capture data under highly-controlled conditions in the field, along with the distances between these elements used for the "observation" of hydrogeological parameters. It includes the head of the Santiuste basin´s managed aquifer recharge system and the ZNS-1 station. The table in the right-upper corner provides the position of the main units. WGS 84. Time Zone 30. Sig-pac plot of land 40:221:0:0:1:6244 (https://sigpac.mapa.es/fega/visor/).

Fig. 4 - Schema degli elementi chiave disponibili per l'acquisizione di dati in condizioni altamente controllate sul campo, insieme alle distanze tra questi elementi utilizzate per l'"osservazione" dei parametri idrogeologici. Include la testa del sistema di ricarica gestita dell'acquifero del bacino di Santiuste e la stazione ZNS-1. La tabella nell'angolo superiore destro fornisce la posizione delle unità principali. WGS 84. Fuso Orario 30. Tracciato Sig-pac del terreno 40:221:0:0:1:6244 (https://sigpac.mapa.es/fega/visor/).

progression of the humidification front, and to determine when water from the channel reaches the deepest sensor through the unsaturated zone. Placing the sensors at different depths allows for precise measurements of the time it takes for rainfall (measured at the Inforiego SG-02 station) to reach the first sensor. This is important for for water balance, distinguishing between infiltrated water from precipitation and artificial recharge. The second (deepest) sensor provides accurate measurements of vertical hydraulic conductivities in the unsaturated zone.

Associated with station ZNS-1, the piezometer 1 was constructed and equipped on 12/11/2020. Both, the piezometer and the deepest sensor of the ZNS-1 station are placed perpendicular to the groundwater flow lines. The distance between the channel and sensor ZNS-1 (installed in October 2008) is 38 meters, while the distance between the channel and piezometer's sensor 1 is 19.70 meters (Fig. 4). Both, (the CTD sensor and moisture-thermometer) are located at a depth of 2.10 meters (about 30 cm lower than the channel´s bottom) (Fig. 5) (MARSOL, 2016a). The calculated horizontal permeability is equated to K_y.

In regards to the artificial recharge infiltration pond, the hydrodynamic process happens in the following way. At the beginning of each artificial recharge cycle, the water derived from the Voltoya River flows into a 14,322 m^2 stagnation and infiltration pond (Fernández, 2014). The intentional recharge then begins, creating a humidification bulb with a mainly vertical component (simplifying the behaviour). The recharge water descends towards the water table, located approximately 3.75 meters (2008, October, Table additional materials (A.M.1) below the surface (Fig. 5). Once the system reaches "vertical control", the main progression of the humidification bulb becomes horizontal and radial from the basin's banks, depending on the permeabilities of the receiving medium, and the direction of advance, as observed in the field (see results). This progression is greater in the south-north direction, matching the groundwater flow in the NNE direction (MAPA, 2005), than in the east-west direction.
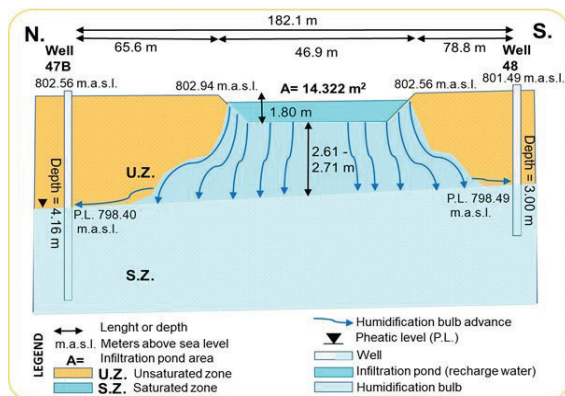

Fig. 5 - Santiuste MAR system's infiltration pond. Profile exposing its response to artificial recharge, main elements and distances for data collection and calculations.

Fig. 5 - Bacino di infiltrazione del sistema MAR di Santiuste. Profilo che mostra la risposta alla ricarica artificiale, gli elementi e le distanze principali per la raccolta dati e i calcoli.

In regards to the artificial recharge in the West Channel, once the water from the infiltration pond flows over the concrete weir into the west channel, it travels through the channel at a level 1.80 m below the average ground level on the west bank service road. This creates a humidification bulb, with a semi-vertical main component until it reaches the water table (see Table A.M. 1, column fifth). After reaching "vertical control", bilateral (east-west) displacement occurs from both sides of the channel, recharging the unsaturated zone, and progressing towards the piezometer 1's sensor and the deepest sensor of ZNS-1, both located at the depth of 2.10 meters. To saturate both sensors, water is required to fill the unsaturated zone space between the previous water table and the depth of 2.10-meters, spanning a distance of 38 meters between the west channel's wetted perimeter and the deepest ZNS-1 sensor (Fig. 6). In continuous MAR cycles, if artificial recharge began on November 1st, the bulb saturated the deepest ZNS-1 sensor about a week later, depending on the accumulation of gas clogging (MARSOL, 2016 a-b).

By calculating the time when the bulb component is mainly horizontal, after saturating the volume of the unsaturated zone under the sensors, the horizontal permeability (comparable to K_y), has been determined (see Table A.M. 1 in the additional materials section). Once the sensor is saturated, the dynamic level generated by the humidification bulb can reach about 1.40 meters depth in "lateral control". This is equivalent to the maximum water level in the artificial recharge West channel. This condition is observed during the wettest recharge cycles, when the volume from the Voltoya River for recharge exceeds approximately 3.5 Mm^3 (Fig. 6).
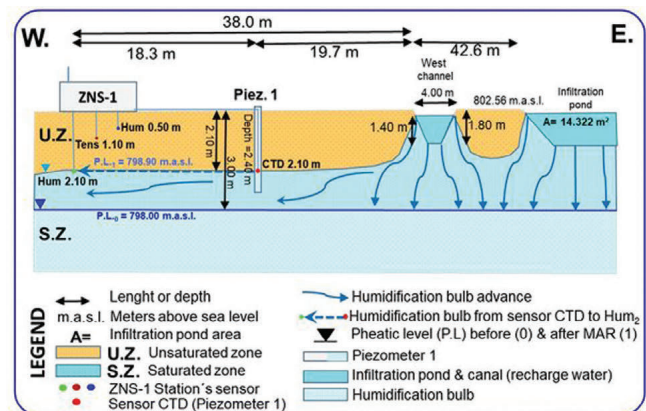

Fig. 6 - Santiuste MAR system west channel. Profile exposing the main elements and distances for data gathering and calculations. Scheme for the cross-section representation of the humidification bulb's advance from the infiltration basin and West channel. Range of the CTD sensor in piezometer 1 (2.10 m), and the deepest sensor (humidimeter 2) of ZNS-1 (2.10 m), 18.3 m away. The depth of the channel's lowest point is 1.80 m. The water depth in the channel typically varies from 60 cm to 140 cm.

Fig. 6 - Canale ovest del sistema MAR di Santiuste. Profilo che mostra gli elementi e le distanze principali per la raccolta dati e i calcoli. Schema per la rappresentazione della sezione trasversale dell'avanzamento del bulbo di umidificazione dalla vasca di infiltrazione e dal canale ovest. Portata del sensore CTD nel piezometro 1 (2.10 m) e del sensore più profondo (igrometro 2) di ZNS-1 (2.10 m), a 18.3 m di distanza. La profondità del punto più basso del canale è di 1.80 m. La profondità dell'acqua nel canale varia tipicamente da 60 cm a 140 cm.

Methods for K$_z$ calculation

Rainfall after precipitation. time taken from zns-1 sensor 1 to sensor 2

The rainwater precipitated inside ZNS-1 station (considering the values monitored by the Nava de la Asunción Meteo Station SG-02) begins its vertical infiltration, leading to an increase in humidity. This is detected first by the sensor situated 0.50 m deep, and then by the second sensor located 2.10 m deep. The time interval between both detections is recorded by the data logger, which possibilities to calculate different K$_z$ values for each instance of rain. K$_z$ represents the relationship between 1.60 m and the time interval between both rises in humidity (see Figure 7 and Table A.M. 2). This calculation requires a prolonged dry period prior to the rain event in order to observe significant changes in humidity detected by the sensors. The precipitations data for the first week of each recharge cycle is presented in Table A.M. 7. The sensors were installed through oblique auger-drilled conduits, which lowers the risk of material remobilization in vertical downward paths, although the infiltration rate may be oversized as the water passes through the sections created by the auger.
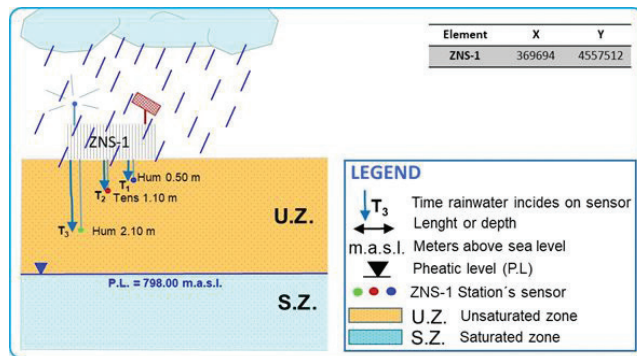

Fig. 7 - ZNS-1 station and sensors used to calculate the vertical infiltration rate when rainwater passes through the entire length of inter-humidimeters.

Fig. 7 - Stazione ZNS-1 e sensori utilizzati per calcolare il tasso di infiltrazione verticale quando l'acqua piovana passa attraverso l'intera lunghezza tra gli igrometri.

In-person data gathering methods

The remaining methodology is reliant on gathering data in person and includes:

Double ring infiltration tests

An automatic measurement method is proposed to streamline the laborious and repetitive task of measuring water levels by utilizing optical assessment. The designed routine involves placing a water-level meter within the inner ring of the double-ring infiltrometer. The top of the device is secured to a stick or steel bar to keep it stable. The water level meter is connected to a data logger, and the water level readings are automatically recorded. It is crucial to carefully maintain the appropriate water levels within the rings while conducting the test.

Eight different campaigns were conducted from October 2020 to November 2022 (MARSOLUT, 2023a). The data collected were precise to the millimetre and recorded in a data logger in digital format. This reduced the risks of introducing errors during the capture and processing of the information when done manually.

The sensors utilized to track the water level evolution were Hydros 21 water level meter (Fig. 5c). These sensors have a resolution of 1 mm and also provide continuous readings of temperature and electrical conductivity. The sensors are connected to a Decagon ZL6 data logger, which can accommodate up to six sensors simultaneously, and has a minimum sampling frequency of 2 minutes over an approximately 8-hour infiltration test period (Fig. 8).
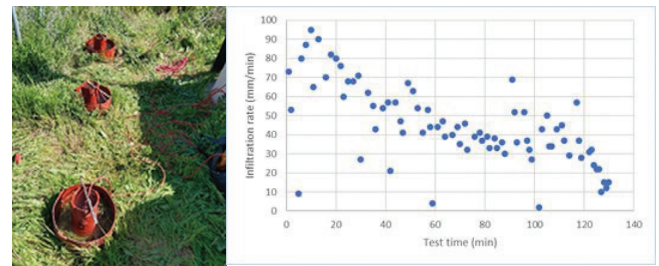

Fig. 8 - Infiltration test conducted using a double-ring infiltrometer. Data collection using a CTD sensor of millimetre accuracy at station ZNS-1. 2021 August 16th (a). Graphical representation of the data (b).

Fig. 8 - Test di infiltrazione condotto utilizzando un infiltrometro a doppio anello. Raccolta dati effettuata tramite un sensore CTD con precisione millimetrica presso la stazione ZNS-1. 16 agosto 2021 (a). Rappresentazione grafica dei dati (b).

The hydraulic conductivity (K) is determined from the charts after the curve trend is obtained during a minimum of four hours of testing, according to the ASTM International Standard D 3385-03, which describes the "Standard Test Method for Infiltration Rates of Soils in the field using Double Ring Infiltrometer" (ASTM, 2018). The results section will display the obtained values.

Slug Tests

The Slug tests conducted in the piezometers 1, STR-1, and STC-1, were done to measure infiltration rates at different depths: next to the ZNS-1 station (piezometer 1), and inside the infiltration pond (piezometers STR-1 and STC-1) (Fig. 9). The main characteristics of these piezometers and tests, adapted from classical slug test to MAR conditions (Henao et al., 2022), are summarized in Table 2. To conduct the slug tests, three piezometers were installed by vertically drilling and inserting a nearly 3-meter long two-inch pipe. The pipe was slotted differently for each piezometer: fully slotted, fully blank, and slotted only at the bottom. These configurations allowed for the estimation of different hydraulic conductivities (K$_{xyz}$) under different saturation conditions: unsaturated (slug 1 test type), partially saturated (slug 2), and fully saturated (K$_z$, slug 3) (IGME, 2015; Henao et al., 2022). The configurations of the three piezometers are illustrated in Fig. 9.

Eight different campaigns were conducted from October 2020 to November 2022 (Henao et al., 2022). Data are collected from the data logger in digital format and millimetre accuracy, avoiding the risks of introducing errors during the input data and processing the information if it were to be done manually.
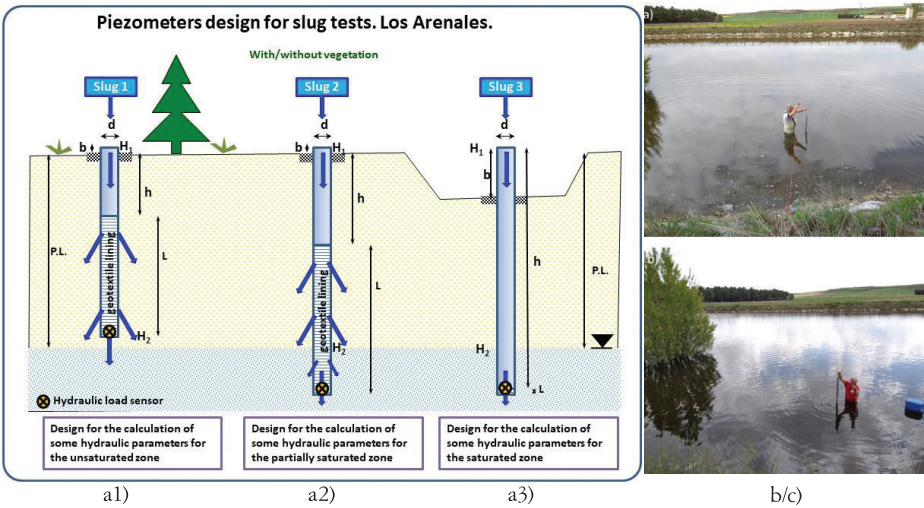
Fig. 9 - Design of three different piezometers constructed for hydraulic parameters calculation (especially K_v) in three different zones: the unsaturated zone (a1), the partially saturated zone (a2), and the completely saturated zone (a3). a2 and a3 were drilled at the bottom of the infiltration pond (taken from MARSOLUT, 2021) (a). Captures were taken during slug tests type 3 (b,c).

Fig. 9 - Configurazione di tre diversi piezometri costruiti per il calcolo dei parametri idraulici (in particolare K_v) in tre diverse zone: la zona non satura (a1), la zona parzialmente satura (a2) e la zona completamente satura (a3). a2 e a3 sono stati perforati sul fondo della vasca di infiltrazione (tratto da MARSOLUT, 2021) (a). Le acquisizioni sono state effettuate durante prove slug test di tipo 3 (b,c).

A Hydrus 21 water level CTR sensor (IMKO, 2016) was inserted into the bottom of the piezometers for the slug tests. This device was set to take measurements every minute. After positioning the sensor and obtaining several initial water table data, water was introduced up to the wellhead, and then, waiting for a period from 30 to 45 minutes, in general, for the water level to fall to the bottom.

Input data were interpreted using SlugIn 1.0 software (IGME, 2015).

Multivariate statistical analysis from data gathering methods

A multivariate statistical analysis was performed with these data to encompass the simultaneous observations and analysis of the different variables, and their relations (Johnson and Wichern, 2007; Rodgers and Nicewander, 1988). The automatic method applied has been the one of the Comillas University (iMAT, 2024). Several attempts to formulate a new equation have been conducted using a Phyton script from the correlation variables matrix and the multivariable probability distribution. These coefficients have been compared to empirical data gathering.

The results of the linear and multiple regressions to determine the most appropriate equation that fits the best results after comparing hydraulic parameters obtained with information given by the sensors, and the ranking of the rest, is exposed in the results chapter.

It is worth to mention that the very precise descriptions have been set out in line with the accuracy required to meet the objectives of the article.

Results

Field data taken under intensely monitored conditions

Objectives 1 and 2: Quantification of the infiltration rates (H and V) and study of the humidification bulb's asymmetry.

In order to expose results in a concise way, the measured values from the field work might not be of interest for the results of this manuscript. Therefore, the data tables have been included at the end of the article (Additional materials, field work data tables, apart from the annex 1 that explains the different formulas).

Arrival of the humidification bulb at wells 47b and 48 (k_x calculation)

To calculate the horizontal hydraulic conductivity, the days required to saturate the space under the infiltration basin, when the change of the principal component of the humidification bulb displacement takes place (from vertical to horizontal), are about 3.5 days. This period must be discounted for the K_h calculation (Table additional materials 1, fifth column). The distance from well 47B to the nearest shore of the pond is 65.60 meters, and to well 48 it is 78.80 meters. Both cross the shallow sandy aquifer (Arévalo Formation).

Well 47B: The "observed" K_x were 20.95, 18.74 and 20.45 m/day for the three observed recharge cycles (A.H. 2008/09, 2014/15, and 2017/18), respectively (Table A.M. 1, rows second to fifth). The mean is 20.05 m/day.

Well 48: Observed K_x were 24.00, 23.30 and 26.00 m/day for the same respective cycles, with a mean of 24.43 m/day (Table A.M. 1, rows sixth to nineth).

Tab. 2 - Information about the new constructed piezometers during 2020. UTM Coordinates, Time Zone 30, ellipsoid WGS 84.

Tab. 2 - Informazioni sui nuovi piezometri realizzati durante il 2020. Coordinate UTM, Time Zone 30, ellissoide WGS 84.

Code	X	Y	Diameter (mm)	Slotted	Deep (m)	Slug Type (1, 2, 3)	Location
Piez 1	369694	4557512	51	Yes	2.55-	Slug 1-2 (unsat-semisat)*	Next to ZNS-1
Piez STR	359916	4557408	51	Yes	2.90	Slug 2 (semisat)	Santiuste inf. pond
Piez STC	359897	4557421	51	Yes	2.93	Slug 3 (sat)	Santiuste inf. pond

Horizontal permeability among artificial recharge channel, deepest zns-1 sensor, and piezometer 1 (ctd sensor) (K_y calculation)

Before constructing piezometer 1, the authors measured the reaction time from the west channel and the deep sensor at station ZNS-1 during 12 recharge cycles between 2008 and 2022 (Table 3, rows ten to 23rd). AH 2011/12 and 2018/19 had no recharge (Fig. 2). The average K_y was found to be 16.65 m/day.

After constructing piezometer 1, and in parallel to the previous calculation, the reaction time between the recharge water from the west channel and the CTD sensor of piezometer 1 was measured. A new K_y was obtained (Table A.M. 1, rows 24th to 27th), yielding an average result of 17.35 m/day from 2020, when the sensor was installed, until 2022.

The calculations of these hydraulic conductivities were conducted under different environmental conditions of humidity, temperature, and capillary tension, from the beginning of the artificial recharge's cycle until the saturation of the sensors (Additional materials, Table A.M. 1). Years with data recording failures have been noted with N/A; and those with no measurements with X.

Rainwater after precipitation. time taken from zns-1 sensor 1 to sensor 2 (K_z calculation)

The determination of K_z dividing the vertical separation between both humidimeters (0.50 and 2.10 meters deep) might depend on the volume of rainwater precipitated during the previous days.

Initial calculations after setting both sensors (Fig. 7) pose a difference of time of about 8 h 45 min, which entails a K_z in this exact point of about 4.4 m/day. These figures, although above references (between 0.32 and 0.50 m/day, MAPA 2005), are consistent with the double-ring tests´ results performed on the surface of the station ZNS-1 (Fig. 8), and also with the slug tests performed in the piezometer 1 (Fig. 9).

Final results observed under intensely monitored conditions

Table A.M. 2 presents the most reliable results obtained from hydrodynamic monitoring for K_{xyz} at the Santiuste MAR system's head spot. The results expose the time taken for the groundwater flow to move from the infiltration pond to the monitoring wells (K_x, between 20.50 and 24.43 m/day); and from the infiltration channel to sensors (K_y, between 16.65 and 17.35 m/day). K_z between two sensors is 4.4 m/day.

These results have been supported by reliable indirect methods.

Indirect permeability calculations

Pumping test in the well 47B

A pumping test was conducted in the well 47B on 2008 October 8th, before taking a point measurement of bulb arrival from the infiltration pond in the recharge cycle: 2008/09. The P.T. 47B trial had two observation piezometers (A and B) for drawdown and recovery data gathering (Fig. 3).

The initial water table was at 4.31 m depth. It was pumped for 8 hours, and its recovery was controlled. The resulting values after applying three interpretative procedures, rejecting the first one (Theis) for implausible results, were 401 and 496 m²/day for transmissivity, and 21.1 and 17.7 m/day for permeability by the Newman and Hantush methods, respectively. The resulting storage coefficients were 21.1 and 17.7, in the same order.

In the present work, the test has been reinterpreted with three calculation methods for estimating hydrogeological parameters (Theis, Newman and Hantush), which can be considered appropriate for the existing boundary conditions. The results obtained are shown in Table A.M. 3 with K values between 6.17 and 24.80 m/day.

Double ring infiltration tests (K_z calculation)

The hydraulic conductivities (K) obtained in previous references (MARSOL, 2016), and in the five tests performed in ZNS-1 station (Fig. 8) on 4th and 5th May 2022 (Henao, 2023) are exposed in Table A.M. 4. Results for K vary between 2.70 and 24.0 m/day.

Infiltration tests in ditches (K_{yz} calculation)

The infiltration tests in ditches were interpreted using Green & Ampt and Kostiakov equations. The capillary suction calculated for the Green & Ampt is $\Psi_f = 0,923$ (-cm). The infiltration results are not pure K_z because the infiltration through the walls of the ditch, although it has been considered a "K_v" (Table A.M. 5). The results for K range between 0.28 and 30.55 m/day.

Slug tests

The results of the slug tests carried out during the MARSOLut project (MARSOLUT, 2021,2023a, 2023b) have been interpreted by Cooper et al., (Cooper et al., 1967), Hvorslev (Hvorslev, 1951), and Bouwer & Rice (Bouwer & Rice. 1976) methods (MARSOLUT, 2023a). The summary of the results is presented in Table A.M. 6. K varies between 1.76 and 84.32 m/day.

Field data and estimated parameters necessary for the selected equations

The objective 3 is about the use of 20 equations to compare in-field data with the intensely monitored results, what might be considered a "digital twin".

Depending on the type of test to determine the hydraulic parameters, especially the hydraulic conductivities (surface and at different depths, and in the three directions), the necessary data have been collected from the review of every one of the components of the interpretation formulas set out in Table 1 (extended in Annex 1). The results are presented in the following section.

The methodology is usually described in its corresponding standard when it exists, e.g. for Lefranc tests, the ISO 22282-2:2012 standard is used.

To apply all of the selected equations, the system must allow the collection of several data and parameters specified in ANNEX 1 (Necessary data and template design).

Some parameters are determined in the cabinet during interpretation, such as:

‒ The Kraijenhoff van de Leur "completing" function, α_t;

- The Matsuo-Akai coefficient C;
- The Ernst radial resistance Wr;
- The Hvorslev variables k and b;
- The Chapuis correction for wells or piezometers with bottom plugs;
- The hydraulic gradient of Darcy, i;
- The capillary suction capacity, metric pressure or negative pressure around the humidification bulb of Green and Ampt, φ_f;
- The Kostiakov parameters b and m;
- The dimensionless numerical factor K of Lewis.

In addition, all those parameters that must be obtained in the laboratory. The estimation of these parameters have required the entire amount of data previously presented.

Results of the selected equations

The objective 4 pursues an equations ranking according to their accuracy.

The equations from Table 1 have been used with the most accurate available data. The results are exposed in Tables 3 and 4. Due to their interest, they have not been annexed in the additional materials section.

Final trustable indirect results

The most accurate indirect results selected after comparing the formulas with in-field data are extracted in Table 3. Values include the method of interpretation, the interval of variation, some means, and an accurate referenced value.

For comments about these equations, see the "discussion" section.

Ranking of the equations in comparison to real conditions measures

The validity of various equations for the type of aquifer under study (high permeability fine-grained granular), and the accuracy of the results concerning the results obtained in the field (under different environmental conditions and intensively monitored) are exposed in Table 4. Columns fifth and sixth expose the residuals, or differences between measured and calculated data, and column seventh displays the ranking of the selected calculations according to their accuracy (for the specific environmental conditions of the Santiuste basin).

Monitoring of the Living Lab. Data gathering results

To advance in the study of the relationship between hydraulic conductivities and environmental parameters, especially humidity and temperature of the unsaturated zone as it is saturated by the humidification bulb, available data have been gathered in Table A.M. 7 (Additional materials section). The explicit measurements are those taken at the beginning of each artificial recharge cycle (column 3rd). Columns 4th and 5th show the humidity of the unsaturated zone in which the humidification bulb advances horizontally from the infiltration pond or the West channel and firstly reaches the CTD sensor of piezometer 1, and secondly the deepest humidimeter-thermometer of ZNS-1 station (columns 4 and 5). The type of sensors and the parameters obtained have been advanced in the materials and methods section (columns 6th to 11th). Column 12th show the precipitation during the week before the sensor was saturated, and column 13rd include the calculated vertical permeabilities (K_y) for each MAR cycle.

Statistical treatment of data
Data processing

Infiltration rates (expressed as vertical permeabilities) are slightly lower than those evaluated in technical references in nearby points of the aquifer by other methodologies. The values are close to 15 m/day of K_h, 0.5 of K_v (in MAPA, 2005, and leaving their original expression equivalent to K_{xy} and K_z respectively), hydraulic gradient (from 1 to 6%), permeability (from 4 to 5 m /day in the sector of ZNS-1), and transmissivity from 1,200 to 1,400 m²/day. All of them were calculated from the first cycle data beginning the operational stage (Fernández and Merino, 2009).

From the data gathered, three Box-Whisker diagrams (McGill et al., 1978) have been charted from the area around the ZNS-1 station and for the different MAR cycles.

Measurements and parameters

In this sector, the highest conductivities match groundwater flow direction, and this, in turn, with the configuration of the system due to its genetic formation. The highest K_x values have been measured "upward" to the hydraulic gradient, i.e., upstream of the flow lines shown in the hydrogeological mapping, which direction is towards the north-northeast (MOPTMA, 1993).

Tab. 3 - Results obtained from indirect methods more trustable due to their resemblance to intense monitoring, method, intervals and mean values.

Tab. 3 - Risultati ottenuti da metodi indiretti più affidabili dovuti alla maggiore corrispondenza con i dati del monitoraggio intenso, del metodo, agli intervalli e ai valori medi.

	K_x (m/d)	K_y (m/d)	K_h (m/d)	K_v (m/d)	K_z (m/d)	K (m/d)
Pumping test 47B	20.05 (Newman) 24.80 (Hantush)		19.60 (media)			
K_z double ring				4.40-4.60	0.32 − 9.6 (5)	16.8 (MARSOL)
K_v ditch (Green & Ampt)				2.79		
Slug 1-2			14.43 (Cooper et al.)	3.54 (Bouwer & Rice)		
Slug 3					4.22 (Horslev)	

Tab. 4 - Ranking of the compared equations according to their fitness to in-field observations.

Tab. 4 - *Classificazione delle equazioni confrontate in base alla loro aderenza alle osservazioni sul campo.*

| Method	In-field result K (m/day)	Formula's result K (m/day)	Source	Difference (residuals)	Residuals (%)	Ranking
Newman (1975)	19.73	20.05	MAPA, 2009	-0.32	-1.60	1
Hvorslev (1951)*	4.4	4.22	Henao et al. 2022	0.18	4.27	2
Double ring test (ASTM, 2018)	4.4	4.66	MARSOL, 2016 (8 h)	-0.26	-5.58	3
Darcy (1856)*	4.8	4.5	Fernández & Merino, 2009	0.3	6.67	4
Ernst* (1950)	4.8	5.33	Fernández & Senent, 2011	-0.53	-9.94	5
Hantush (1959)	19.73	24.8	MAPA, 2009	-5.07	-20.44	6
Lewis (1937)*	4.4	5.64	Own. K=0.99; N= -0.029	-1.24	-21.99	7
Bouwer & Rice (1976)	4.8	3.54	Henao et al. 2022	1.26	35.59	8
Cooper et al. (1967)	19.73	14.43	Henao et al. 2022	5.3	36.73	9
Jacob (1946)	19.73	34.5	MAPA, 2009	-14.77	-42.81	10
Lefranc (with FF, variable) (Cassan, 2000)	4.66	3.14	MAPA, 2009	1.52	48.41	11
Gilg-Gavard (variable level) (Custodio, 1983)	4.4	8.89	MARSOLUT, 2019	-4.49	-50.51	12
Kostiakov (1932)*	4.8	9.79	MARSOLUT, 2019	-4.99	-50.97	13
Kraijenhoff van de Leur* (1958)	4.4	9.56	Fernández & Senent, 2011	-5.16	-53.97	14
Theis (1935)	19.73	12.63	MAPA, 2009	7.1	56.22	15
Darcy (1856)	4.8	15	MAPA, 1999	-10.2	-68.00	16
Matsuo-Akai* (1952)	4.4	15.66	Own. C= -0.33	-11.26	-71.90	17
Green & Ampt (1911)*	4.8	2.79	Ψ_f = 0,9228 (-cm) MARSOLUT, 2019	2.01	72.04	18
Lefranc (with FF, variable) (Cassan, 2000)	4.66	1.54	MAPA, 1999	3.12	202.60	19
Thiem (1906)	19.73	6.17	MAPA, 2009	13.56	219.77	20

The horizontal permeability (K_h) obtained is about 25% of that from pumping tests in the "upward" direction. The vertical permeability (K_z) around ZNS-1, is one-third of that reported in the background (MAPA, 2005). The hydraulic gradient of the artificial recharge channel "upstream" is about 1% (Fernández et al., 2009).

In the absence of more precise analyses, the asymmetry of the humidification bulb is not remarkable, although it is noticeable. The mean K_x (with reliable data) is 22.40 m/day (rounded values), K_y is 17.00 m/day, and K_z is 4.40 m/day (Table A.M. 2). These values are really high but proper for a

sandy aquifer originally a dune system, like this area is. The clogging effect reduces these parameters.

The evolution of Kh and Kv have been charted in trend diagrams (Fig. 10) for the MAR cycles in which proper campaigns of monitoring and data collection were conducted by direct observation. See original data in Table A.M. 1.

Based on the borehole columns, there are layers of reeds and clays in the most closely monitored area (Fernández & Prieto, 2013). The impact of these layers appears to be significant and may not be applicable to other areas.
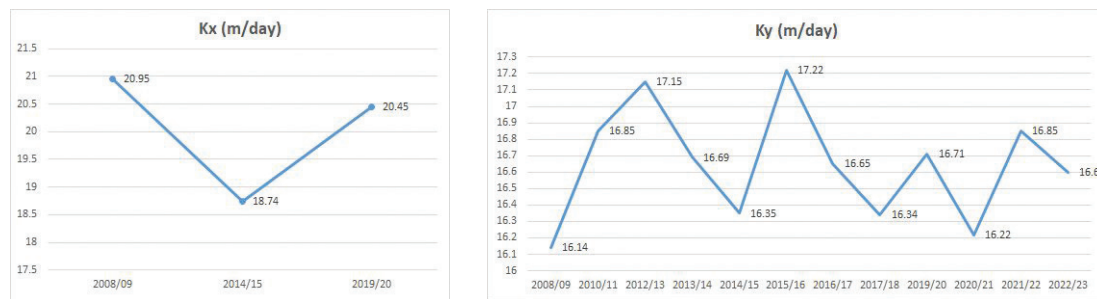
Fig. 10 - Evolution of K_x and K_y (observed in the field) for the different MAR cycles.

Fig. 10 - *Evoluzione di K_x e K_y (osservata in campo) per i differenti cicli di MAR.*

Statistical analysis of data

To statistically analyse the field observations and complement the graphical representation of their trends, box plots diagrams (McGill et al., 1978) have been created for the three cycles of Managed Aquifer Recharge (MAR). K_x data have been gathered from observations conducted between the Infiltration pond and Well 47B (Fig. 11).

K_y data have been collected from observations between the West Channel and the ZNS station's sensors. Intervals from the obtained numerical values have been established (Fig. 12).
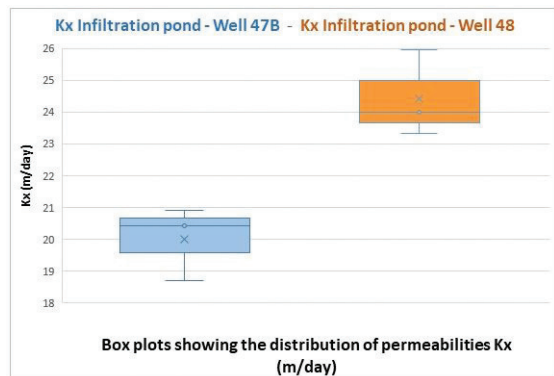
Fig. 11 - Box plots display the permeability distribution (K_x), in m/day, measured under highly controlled conditions between the infiltration pond and the Well 48.

Fig. 11 - Grafici box plot che mostrano la distribuzione della permeabilità (K_x), in m/giorno, misurata in condizioni altamente controllate tra la vasca di infiltrazione e il Pozzo 48.
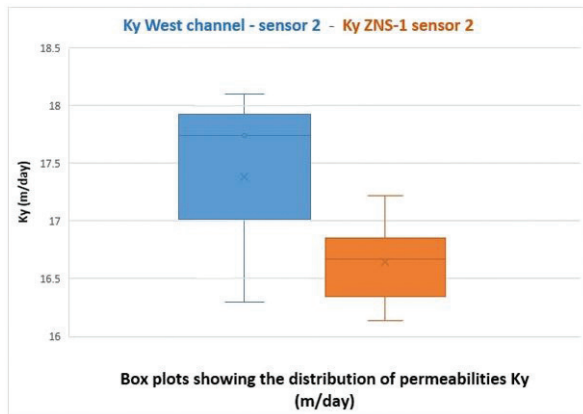

Fig. 12 - Box plots showing the distribution of permeabilities K_y, in m/day, measured under highly-controlled conditions between the West channel and sensor CTD of piezometer 1 (a), and deepest sensor of the ZNS-1 station (b).

Fig. 12 - Grafici box plot che mostrano la distribuzione della permeabilità (K_y), in m/giorno, misurata in condizioni altamente controllate tra il canale ovest e il sensore CTD del piezometro 1 (a), e il sensore più profondo della stazione ZNS-1 (b).

Ranking of the equations in comparison to real conditions measures

With the data obtained under "hyper-controlled" conditions, and once the precise time for the wetting bulb to reach each humidimeter from the recharge channel has been determined, observed results have been compared with the permeability results of some (the most successful) of the theoretical equations, considering the spacing between drains as the distance in the horizontal between the bottom of the channel and the position of the sensors, and the thicknesses as those measured in the field.

According to the aggregation of the different interpretation methods (Table 1), selected approaches have been discussed:

Group 1ab

The most precise has been the tests with a double ring infiltrometer. The values about 4.60 m/day for K_v match well the in-the-field permeabilities. K_h values range between 9.60 and 24 m/day, which are acceptable results. Notice the minimum duration of each test was 8 hours, requiring huge volumes of water.

Tests using the Lefranc and Gilg-Gavard equations for the variable hydraulic load (1b) (ISO, 2012) gave results about two orders of magnitude lower than those measured in the field.

Group 2ab

The Ernst equation (Ernst, 1950) is specific to steady-state flow calculations in stratified soils where the upper layer usually has lower permeability than the underlying stratum. It considers four flow components: vertical, horizontal, radial, and an additional inflow attributable to artificial recharge. Therefore, its degree of certainty may be questioned for the environmental circumstances of this experience.

The radial flow discharge component, which would be the most comparable to the expansion of the humidification bulb at the bottom of the channels, is directly proportional to the head losses, and inversely proportional to the radial resistance (Fernández, 2005). The result applying this equation for station ZNS-1 shows some divergence with the in situ measurements. In the case of Ernst, the radial resistance obtained from Ernst's abacus is close to 5.50 d/m. If we consider Wr the unknown parameter, its magnitude can be estimated by clearing it in the equation and giving h the measured value. In this case, the result is 5.33 m/d.

Equating the radial flow region to the humidification bulb, the flow through the ZNS-1 station is found to differ by even about seven times, e.g. results from Jacob and Ernst methods. Also, vertical permeability is quite higher (about double) for measurement under highly-controlled conditions, e.g. for Green & Ampt vs double ring infiltrometer results.

The Kraijenhoff van de Leur equation (Kraijenhoff Van de Leur, 1958), derived for the variable regime, takes into account the recharge attributable to irrigation and rainwater, and allows prediction of the oscillation and position of the water table as a function of the rainfall pattern, hydraulic parameters of the aquifer, and the drainage system. It is applied in more homogeneous soils and deep aquifers, so, in this context it is necessary to introduce the Dupuit's simplifications for horizontal flow (Dupuit, 1857). The equation considers constant rainfall (assimilable to artificial recharge) and that the aquifer has reached steady-state functioning. The vertical flow obtained by applying the Kraijenhoff van de Leur equation is about 9.56 m/d, about twice that obtained in the field.

The permeability after applying the Lewis equation (Lewis, 1937) results in -5.64 m/day. The specific parameters adopted have been: K=0.99; N= -0.029. Both might be considered estimations, and the final result is the absolute value of the equation's output.

Matsuo-Akai equation (Matsuo-Akai, 1952) output exaggerated results of about four times the field observations, using an authors´ estimation for the C coefficient, C= -0.33, which differs for different environmental conditions.

Group 3. Slug tests

In regards to Slug tests and the three methods tested for interpretation, Hvorslev's formula (Hvorslev, 1951) has given exceptionally accurate results, with a mean K_z of 4.22 m/day, the closest to the results measured in the field for the study area (4,4 m/day). Two tests from one campaign were rejected because of negative hydraulic properties. It exceeds about 13x the double ring infiltrometer results.

The Bouwer & Rice method (Bouwer & Rice, 1976) provided permeability values consistent with expectations. The Cooper et al. method (Cooper et al., 1967) gave negative values in two campaigns out of four. Infiltration rates averaged about 2.6 m/day. These values are within the order of magnitude of the Santiuste basin, and they are generally lower than those measured at the surface using double rings.

Group 4. Indirect methods

The most accurate result was the pumping test interpreted by Newman's equation (Neuman, 1975), with a mean value (K_{xy}) of about 20.05 m/day, just between K_x and K_y values observed in the field.

The remaining equations generally require parameters that are difficult to obtain in the field. The theoretical values introduce a large uncertainty into the calculation process. The methods that have yielded values closest to the monitoring observations have been listed and ranked in Table 4.

Analysis of the environmental data and their trends from hydrodynamic monitoring

The analysis of the results has been conducted mainly through the study of statistical diagrams and the trend evolution in the various graphs created using the in-field measured parameters (Table A.M. 7).

K, H and T relationships

The relations between the West channel and the ZNS-1's deepest sensor have allowed to stablish permeability ranges based on the different monitored parameters, i.e., humidity, temperature, capillary tension (captured by ZNS-1's sensors), and total precipitations during the previous week (recorded in the Inforiego station SG02, Nava de la Asunción) (Fig. 13).

Available data of humidity, temperature, and capillary tension have been plotted in a Box-Whisker diagram (McGill et al., 1978), as well as precipitation during the week before each MAR cycle (Fig. 14).
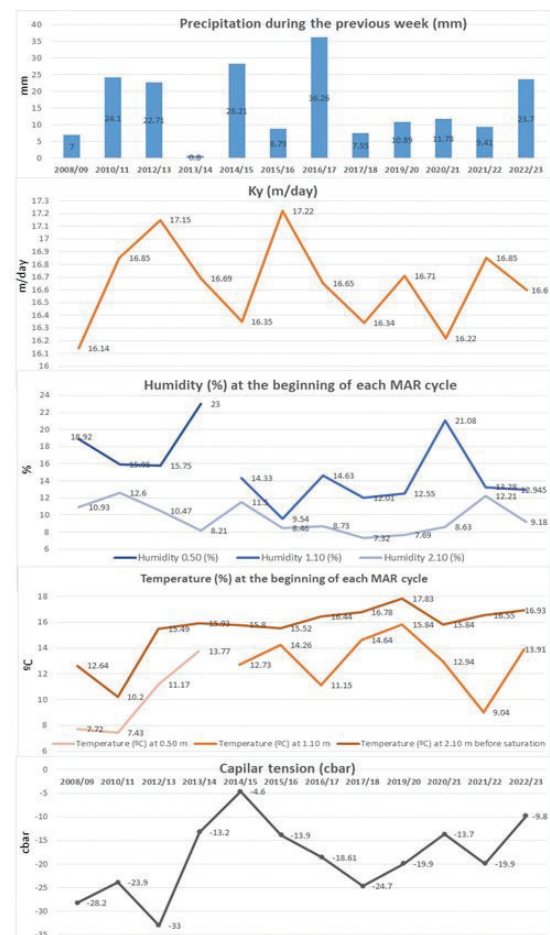

Fig. 13 - Relation between permeabilities and unsaturated zone parameters: humidity, temperature, and capillary tension, captured by ZNS-1's sensors, during the period in which the humidification bulb saturated the piezometer 1 CTD sensor and the ZNS-1 deepest sensor. Precipitations during the week before the MAR cycles began are in the top.

Fig. 13 - Relazione tra permeabilità e parametri della zona non satura: umidità, temperatura e tensione capillare, acquisiti dai sensori di ZNS-1, durante il periodo in cui il bulbo di umidificazione ha saturato il sensore CTD del piezometro 1 e il sensore più profondo di ZNS-1. Le precipitazioni durante la settimana precedente all'inizio dei cicli MAR sono nella parte superiore.
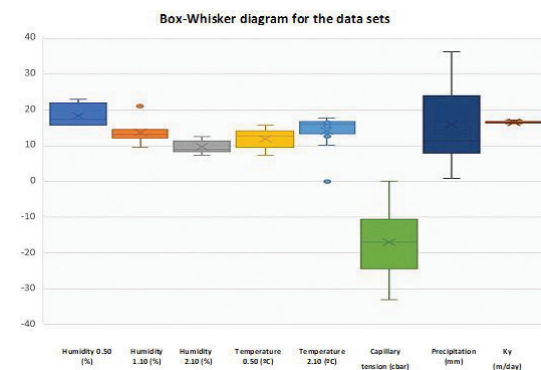

Fig. 14 - Box-Whisker plots representing the statistical treatment of humidity, temperature, and capillary tension data recorded at ZNS-1 station, along with precipitation data registered from the close SG02 Meteo station.

Fig. 14 - Diagrammi a scatola e baffi che rappresentano il trattamento statistico dei dati di umidità, temperatura e tensione capillare registrati presso la stazione ZNS-1, insieme ai dati di precipitazione registrati dalla vicina stazione meteo SG02.
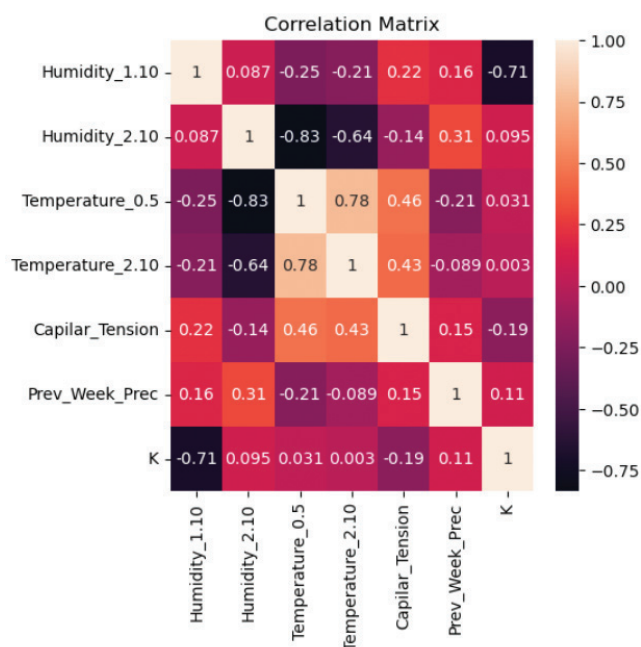
Fig. 15 - Correlation matrix among the sensor's data gathered, including precipitation of the week prior to the intentional recharge cycle began, versus mean permeability (K).

Fig. 15 - Matrice di correlazione tra i dati acquisiti dai sensori, inclusa la precipitazione della settimana precedente all'inizio del ciclo di ricarica intenzionale, rispetto alla permeabilità media (K).

Multivariable statistical analysis and results

Multivariate statistical analysis has been posed with these data, applying the Multicorrelation_PRyES_v1.7 method (chapter 5). It has provided the following results (Fig. 15).

The correlation among hydraulic conductivity, humidity, temperature, capillary tension and recent precipitation follows a scale between -1 and +1, where a negative value indicates an inverse correlation and a positive value indicates a direct correlation. The closer the value is to the extremes, the stronger the correlation, while values nearing zero indicate independent variables. A high or moderate inverse correlation can be observed between temperatures (Temperature_0.5, Temperature_2.10) and humidity (Humidity_2.10). Additionally, there is a moderate direct correlation between the temperatures, also with temperatures and capillary tension.

Concerning the correlation of permeability, it is almost negligible for all variables except for Humidity_1.10, where a high inverse correlation is observed with a value of -0.71. This suggests that as humidity increases, permeability tends to decrease, and vice versa. The strong negative correlation observed implies a consistent inverse trend between these variables across the dataset. In many contexts, this relationship is logical. For instance, in porous materials or certain soil types, increased humidity can fill the pores and pathways, reducing the material's permeability. Additionally, materials that compact when saturated often exhibit decreased permeability with higher moisture levels.

Discussion

A trends analysis that included data on humidity, temperature, and capillary tension has been conducted. All of them were collected throughout the artificial recharge cycles at the Santiuste ZNS-1 station, adjacent to the West channel. Additionally, the circulating flow, precipitation and ambient temperature have been monitored, allowing correlating these parameters on a daily scale.

Based on the trend study with a time scale of each first week of each artificial recharge cycle), an immediate response of the moisture gauges to rainfall is observed. The shallowest sensors (0.5 m) show a very rapid response, whilst the deeper ones show delays of up to 3-4 days, with much milder variations. The effect of snow shows a longer delay of more than one week between the recording of precipitation and the response of the humidity analyser.

In all cases, anomalous humidity readings were observed to be very different from the daily average, even though all parameters indicated that the instrument was measuring accurately. These data are attributable to the influence of heavy rainfall, and an unusual response during the saturation process of the deepest sensor, registering an abrupt drop prior to subsequent rise. This immediate change is attributed to the mobilisation of air in the unsaturated zone of the aquifer due to water buoyancy, or upward force equals to the amount of the weight of fluid displaced by the body volume.

The temperature at 0.5 metres shows strong oscillations with a direct proportional relationship to precipitation. It correlates, in general, inversely with humidity. At ZNS-1 the trend is downward as the humidification bulb progresses, until the deep sensor becomes saturated. The temperature recorded at the sensors correlates inversely with increases in humidity.

The capillary tension at a depth of 1.10 m generally decreases with precipitation. The graph shows a valley, which aligns with the two days prior to reaching the 2.10 m humidimeter by the humidification bulb. The capillary tension also experiences an abrupt rise and then fall, possibly due to the arrival of the humidification bulb and its compression of the air in the unsaturated zone, followed by immediate expansion. Overall, a decrease in capillary tension is observed around two days after precipitation, according to monitored data and the non-linear relationship between capillary tension and hydraulic conductivity, as there is not direct correlation. Ensuring this fact would require the application of additional techniques, such as gas chamber sampling and lysimeters.

Regarding the correlation of permeability, the impact of all variables is almost negligible, except for Humidity_1.10, where a high inverse correlation is observed with a value of -0.71. This suggests that as humidity increases, hydraulic conductivity tends to decrease, and vice versa. The strong negative correlation observed implies a consistent inverse trend between these variables across the dataset. In many contexts, this relationship is logical. For instance, in porous materials or certain types of soil, higher soil water content can fill the pores and pathways, which reduces the material's

permeability (Custodio, 1986). Additionally, materials that become compact when saturated often show decreased permeability at higher moisture levels.

According to the results chapter, the observed correlation is both, meaningful and expected in scenarios where humidity significantly impacts a material's ability to transmit fluids.

Based on highly reliable field measurements, and their comparison with the result of applying different equations with the "digital twin" methodology, the parameters of the best-performing equations have been analysed, ranking the results according to their "residuals" accuracy.

Measurements in the observation piezometers as the humidification bulb thrives from the channels and the artificial recharge basin laterally confirm its asymmetric morphology. It presents a steeper slope against the natural hydraulic gradient, and a very steep and slightly convex-concave profile until the dynamic level is reached.

The application of the equations for the ZNS-1 station nearby area shows some variance from the in situ measurements.

The inflow and residual hydraulic load obtained from applying the equations of Ernst, Kraijenhoff van de Leur, and their comparison with the in-field observed and recorded aquifer storage variation, show an unsatisfactory similarity in both cases. The Kraijenhoff van de Leur equation has yielded flux measurements of more than twice the measured values, with a residual close to 7 m/d. This may be because the boundary conditions are not similar to those proposed by the authors and that applied formulae are simplified.

At this point, simple equations are used that handle quantifiable parameters in the field, with specific corrections designed "à la carte" for each aquifer. In the case of Santiuste, the most successful methodologies have been: Bouwer and Rice for slug tests, Newman for pumping tests, Norma ASTM D3385-18 for double-ring infiltration tests, and Green & Ampt for tests in small trenches.

The recording of humidity, temperature, conductivity and capillary tension data collected over several artificial recharge cycles in the sector, during the days on which the arrival of the humidification bulb at the sensors occurs, also requires knowledge of other exogenous data. These include the flow rate through the pipes, precipitation, ambient temperature, etc. These allow for improving the correlations among these parameters daily, especially the previous precipitation at least in the previous week. The correlations between representative parameters show reasonable degrees of adjustment.

In general, there is an immediate response from the humidity sensors installed in the ZNS station after rainfall. Temperature has a certain inverse correlation with humidity increases. Capillary tension shows a generally decreasing trend with precipitation.

The use of IT technologies for permeability appraisal significantly enhances accuracy and efficiency in data analysis. Advanced software and scripts, such as the one used "Multicorrelation_PRyES_v1.7", enable the processing of large datasets and the application of statistical models. These technologies facilitate the generation of visual correlation matrices, which provide clear and intuitive insights into the relationships between variables. Consequently, this leads to more precise permeability assessments, aiding in the identification of patterns and trends that traditional methods might miss.

Conclusions

These research findings might be useful to select the best formula to determine certain hydraulic characteristics in certain hydrogeological studies, specifically in MAR areas placed on granular aquifers. The proposal for one unique equation for groundwater flow in an specific area gives a future direction for research.

This aquifer has traditionally been considered a highly homogeneous and isotropic medium. However, due to the hydraulic characteristics, there is a notable difference between horizontal and vertical permeability, especially in areas with layers of gravel and clay. Therefore, the idea that the Los Arenales aquifer is completely uniform and consistent is not accurate and it is necessary to differentiate between K_x, K_y, and K_z, avoiding assumptions of isotropy. The value of this parameter is found to be dependent on the degree of soil saturation, precipitation, humidity, and soil temperature, without a clear correlation with unsaturated capillary tension.

Even though the differences are slight, we can distinguish between K_x, K_y, and K_z for unsaturated, semi-saturated, and saturated conditions, making it more complicated to determine the ideal parameters in the field, as they are somewhat reliant on environmental conditions.

The dispersion of the data has also impeded the determination of an accurate new equation after several tests, which entails difficulties in proposing a groundwater movement equation around the head of Santiuste Basin's MAR system, and many others. Therefore, to find one unique equation for groundwater flow in a large area is, indeed, challenging.

REFERENCES

ASTM (2018) ASTM D3385-18 Standard Test Method For Infiltration Rate of Soils in Field Using Double-Ring Infiltrometer. ASTM International.

Bouwer, H. y Rice, R.C. (1976). A slug test for determining hydraulic conductivity of unconfined aquifers with completely or partially penetrating wells. Water Resources Res. Vol. 12 (3), 423-428.

Bouwer, H. (1989). Discussion of the Bouwer and Rice slug test-an update. Ground Water, vol. 27(3), 304-309.

Bouwer, H. (1999). Artificial recharge of groundwater: Systems, design, and management. In: Mays LW (ed.) Hydraulic design handbook. McGraw-Hill, New York, pp 24.1–24.44

Bouwer, H. (2002). Artificial recharge of groundwater: hydrogeology and engineering. Hydrogeol J 10(1):121–142

Cassan, M. (2000). Application des essais Lefranc a l´évaluation du coefficient d'anisotropie hydraulique Del sols aquifers *"Lefranc essays application to evaluate the anisotropy coefficient of aquifers"*. Revue Française de géotechnique, nº 90, 2000, p. 25-43. https://www.geotechnique-journal.org/articles/geotech/pdf/2000/01/geotech2000090p25.pdf - last accessed 22/01/2025.

CIS. (2023). Common Implementation Strategy for the Water Framework Directive and the Floods Directive. Guidance document nº XX (draft). Managed Aquifer Recharge (MAR) under the Water Framework Directive. Available online at: https://circabc.europa.eu/ui/group/9ab5926d-bed4-4322-9aa7-9964bbe8312d/library/009c6b9f-3773-4592-ad79-3503dbf6d07f/details

Comillas Pontifical University, iMAT. (2024). Ingeniería Matemática e Inteligencia Artificial (iMAT). *"Mathematical engineering and artificial intelligence"*. Department of Statistics. ICAI. https://www.gradomania.com/grado-en-ingenieria-matematica-e-inteligencia-artificial-madrid-320618_q08.html - last accessed 22/01/2025.

Cooper, HH Jr, Jacob, CE. (1946). A generalized graphical method for evaluating formation constants and summarizing well field history. Trans Am Geophys Union 27 526–534. https://doi.org/10.1029/TR027i004p00526 - last accessed 22/01/2025.

Cooper, H.H., Bredehoeft, J.D. y Papadopulos, S.S. (1967). Response of a finite-diameter well to an Instantaneous charge of water. Water Resources Research. Vol. 3, 263-269.

Custodio, E & Llamas, M.R. (1983). (EDS.). Hidráulica de captaciones de agua subterránea *"Groundwater abstraction hydraulics"*. In: Hidrología Subterránea (Groundwater Hydrology), pp. 969-981. Ed. Omega, 2 Vols., 2,350 pp.

Custodio, E. (1986). "Recarga artificial de acuíferos." *"Artificial recharge of aquifers"*. Boletín de Informaciones y Estudios, nº 45. Servicio Geológico, Ministerio de Obras Públicas y Urbanismo (MOPU). Madrid. 148 pg.

Darcy, H. (1856). Les fontaines publiques de la ville de Dijon *"Public fountains in the city of Dijon"*. Dijon, París 1856.

DINA-MAR. (2010). DINA-MAR: La gestión de la recarga de acuíferos en el marco del desarrollo sostenible. Desarrollo tecnológico *"Management aquifer recharge in the framework of sustainable development. Technological development"*. Grafinat, Madrid, Spain. ISBN 978-84-614-5123-4. Editor: Fernández Escalante, E. https://dinamar.tragsa.es/pdf/dina-mar-2007-2011-libro.pdf - last accessed 22/01/2025.

Dillon, P., Stuyfzand, P., Grischek, T. et al. (2019). Sixty years of global progress in managed aquifer recharge. Hydrogeol J 27, 1–30. 2019. https://doi.org/10.1007/s10040-018-1841-z

Dupuit, J. (1857). Mouvement de l'eau a travers le terrains permeables *"Water movement through permeable ground"*. C. R. Hebd. Seances Acad. 459 Sci., 45:92–96, 1857.

Ernst, L.F. (1950). A new formula for the calculation of permeability factor with the Auger-hole method. T.N.C. Groningen, 1950. Translated from the Dutch by H. Bouwer, Cornell Univ. Ithaca, N.Y. 1955.

Fernández Escalante, A.E. (2005). Recarga artificial de acuíferos en cuencas fluviales. Aspectos cualitativos y medioambientales. Criterios técnicos derivados de la experiencia en la Cubeta de Santiuste, Segovia *"Artificial recharge of aquifers in river basins. Qualitative and environmental aspects. Technical criteria derived from the experience in the Cubeta de Santiuste (Segovia)"*. PhD Thesis. January 2005. Universidad Complutense de Madrid. ISBN: 84-669-2800-6. https://docta.ucm.es/bitstreams/318ab949-e0fd-49d4-8d2d-81daf56ac26b/download - last accessed 22/01/2025.

Fernández Escalante, A.E. & García Merino, A. (2009). Estudio sobre la evolución de la zona no saturada en las inmediaciones de dispositivos de tipo superficial de gestión de la recarga de acuíferos. Las estaciones DINA-MAR ZNS. Primer ciclo de operatividad *"Study on the evolution of the unsaturated zone in the vicinity of surface aquifer recharge management devices. DINA-MAR ZNS stations. First operational cycle"*. Estudios de la zona no saturada del suelo (Studies of the unsaturated zone of the soil). Vol. IX, ZNS´09. Barcelona 2009. pg. 271-280. ISBN: 978-84-96736-83-2.

Fernández Escalante, A.E., García Asensio, J.M. and Minaya Ovejero, M.J. (2009). Propuestas para la detección y corrección de impactos producidos por procesos colmatantes en el dispositivo de recarga artificial de la Cubeta de Santiuste, Segovia *"Proposals for the detection and correction of impacts caused by clogging processes in the artificial recharge device of the Cubeta de Santiuste, Segovia"*. Boletín Geológico Minero (BGM), Vol. 120, nº 2. IGME. Madrid, Spain. Fernández Escalante, A.E. 2010. Caminitos de Agua. Tres rutas hidrogeológicas en la Provincia de Segovia. Guía de interpretación (Little Water ways. Three hydrogeological routes in the Province of Segovia. Interpretation guide). Colección Hidrogeología hoy. Título 5. Ed. Grafinat. October 2010. ISBN 978-84-614-4944-6, 146 pg. https://dinamar.tragsa.es/pdfs/caminitos%20de%20agua-itinerario.pdf - last accessed 22/01/2025.

Fernández Escalante, A.E. & Senent del Álamo, M. (2011). Nuevos estudios sobre la evolución de la Zona No Saturada en las inmediaciones de canales y balsas de gestión de la recarga del acuífero de los Arenales basados en las estaciones DINA-MAR ZNS *"New studies on the evolution of the Unsaturated Zone in the vicinity of canals and recharge management ponds of the Los Arenales aquifer based on the DINA-MAR ZNS stations"*. Studies of the unsaturated zone of the soil, Vol X. Salamanca (Spain), 2011, October, 19-21. Pg. 315-320. ISBN 978-84-694-6642-1.

Fernández Escalante, A.E. (2013). Practical criteria in the design and maintenance of MAR facilities in order to minimise clogging impacts obtained from two different operative sites in Spain. In: Martin R (ed.) Clogging issues associated with managed aquifer recharge methods. IAH Commission on Managing Aquifer Recharge. 119-154.

Fernández Escalante, A.E., Grupo Tragsa. (2014). 2002-2012, Una década de la recarga gestionada. Acuífero de la Cubeta de Santiuste (Castilla y León) (2002-2012, *"A decade of managed recharge. Cubeta de Santiuste Aquifer (Castile and Leon)"*. Ed. Tragsa. April 2014. Hidrogeología hoy. ISBN 84-616-8910-0. 298 pg. https://dinamar.tragsa.es/pdf/IF-hh7-v34c.pdf - last accessed 22/01/2025.

Fernández-Escalante, A.E., Prieto Leache, I. (2013). Los procesos colmatantes en dispositivos de gestión de la recarga de acuíferos y empleo de la termografía para su detección y estudio. Un ensayo metodológico en el acuífero "Los Arenales", España. *"The clogging processes in aquifer recharge management devices and the use of thermography for their detection and study. A methodological test in the "Los Arenales" Aquifer, Spain"*. Bol. Soc. Geológica Mex. 65, 51–69. http://dx.doi.org/10.18268/BSGM2013v65n1a5 - last accessed 22/01/2025.

Fernández-Escalante, A.E., San Sebastian Sauto, J. (2019). Clogging map for Santiuste basin MAR site, Los Arenales Aquifer, Spain. Multivariable analysis to correlate types of clogging and groundwater quality, in: Managed Aquifer Recharge: Local Solutions to the Global Water Crisis - Proceedings of the Symposium ISMAR 10. Madrid, Spain, pp. 450–463. https://dinamar.tragsa.es/file.axd?file=/PDFS/ISMAR10-proceedings-book_EF.pdf - last accessed 22/01/2025.

Fernández-Escalante, A.E & López-Gunn, E. (2021). Co-managed aquifer recharge: Case studies from Castilla y León (Spain), in: The Role of Sound Groundwater Resources Management and Governance to Achieve Water Security (Series III), Global Water Security Issues (GWSI) Series. UNESCO Publishing, Paris. https://unesdoc.unesco.org/ark:/48223/pf0000379093 - last accessed 22/01/2025.

UN (2022) Concept Note on the Water Action Agenda, Version 1 November 2022. Available from https://sdgs.un.org/conferences/water2023/action-agenda, - last access 15-12-2024

Gómez-Espín, J.M. (2019). Modernización de regadíos en España: experiencias de control, ahorro y eficacia en el uso del agua para riego *"Modernisation of irrigation in Spain: experiences of control, savings and efficiency in the use of water for irrigation"*. Agua Territorio 69–76. https://doi.org/10.17561/at.13.3972 - last accessed 22/01/2025.

Green, W.H. and G. Ampt. (1911). Studies of soil physics, part I – the flow of air and water through soils. Physical Hydrology for Ecosystems. BEE 3710 J. Ag. Sci. 4:1-24.

Guyennon, N., Salerno, F., Portoghese, I., Romano, E. (2017). Climate Change Adaptation in a Mediterranean Semi-Arid Catchment: Testing Managed Aquifer Recharge and Increased Surface Reservoir Capacity. Water 9, 689. https://doi.org/10.3390/w9090689 - last accessed 22/01/2025.

Hantush, M. S. (1959). Nonsteady flow to flowing wells in leaky aquifers, J. Geophys. Research, 64, 1043–1052.

Henao Casas, J.D.; Fernández Escalante, A.E.; Calero Gil, R.; Ayuga, F. (2022). Managed Aquifer Recharge as a Low-Regret Measure for Climate Change Adaptation: Insights from Los Arenales, Spain. Water 2022, 14, 3703. https://doi.org/10.3390/w14223703 - last accessed 22/01/2025.

Henao Casas, J. D., Fernández Escalante, A.E., Ayuga, F. (2022). Alleviating drought and water scarcity in the Mediterranean region through managed aquifer recharge. Hydrogeol J 30, 1685–1699. https://doi.org/10.1007/s10040-022-02513-5 - last accessed 22/01/2025.

Henao Casas, J.D. (2023). Managed aquifer recharge as a low-regret measure for climate change adaptation. Doctoral Thesis. https://oa.upm.es/73999/ - last accessed 22/01/2025.

Hvorslev, J.M. (1951). Time lag and soil permeability in ground water observations. Waterways Experiment Station Corps of Engineers, U.S. ARMY, Vol. 36, 50 p.

IGME. (1982). "Mapa Geológico de España." Escala 1: 50.000. Sheets Olmedo (428), Arévalo (455), Navas de Oro (429), Nava de la Asunción (456). *"Geological map of Spain"*. 2nd Serie. CGS-IMINSA.

IGME (2000). Identificación de acciones y programación de actividades de recarga artificial de acuíferos en las cuencas intercomunitarias *"Identification of actions and programming of activities for artificial recharge of aquifers in intercommunity basins"*. Sahún, B, and Mudillo, J.M., Eds. ISBN 84-7840-390-6.

IGME (2015). SlugIn 1. 0. Aplicación para la interpretación de ensayos Slug. Manual de usuario. *"Slug test interpretation application. User's manual"* ISBN on line: 978-84-7840-984-6. https://www.igme.es/productos_descargas/aplicaciones/Manual_SlugIn.pdf - last accessed 22/01/2025.

IMKO (2016). TRIME®-pico32/63. Sensors with internal TDR-electronics. IMKO GmbH. www.IMKO.de - last accessed 22/01/2025.

IMTA (2017). (EDs) Fernández-Escalante, A.E. and San Sebastián Sauto, J. La recarga gestionada en el acuífero Los Arenales, Castilla y León, España. Soluciones tecnológicas aplicadas al desarrollo rural. Manejo de la recarga de acuíferos: un enfoque hacia Latinoamérica, chapter 22 *"Managed recharge in the Los Arenales aquifer, Castilla y León, Spain. Technological solutions applied to rural development. Aquifer recharge management: an approach to Latin America"*. IMTA, Mexico. https://www.imta.gob.mx/biblioteca/libros_html/manejo-recarga-acuiferos-ehl.pdf - last accessed 22/01/2025.

IRYDA (1991). Proyecto de Asistencia Técnica para el Estudio Hidrogeológico de la Cubeta de Santiuste, Segovia *"Technical Assistance Project for the Hydrogeological Study of the Cubeta de Santiuste, Segovia"*. Unpublished technical report available for consultancy at MAPA library). IRYDA-ITGE.

ISO (2012). Geotechnical investigation and testing - Geohydraulic testing - Part 2: Water permeability tests in a borehole using open systems. International Standard ISO 22282-2:2012. https://cdn.standards.iteh.ai/samples/57723/494adfa282064001a04007b3c0296d71/ISO-22282-2-2012.pdf

ITACYL (2020). Plan de Monitorización de los Cultivos de Regadío en Castilla y León - Resultados de la Encuesta de Cultivos con Datos Acumulados de las Campañas Agrícolas 2011-2018 *"Plan for Monitoring Irrigated Crops in Castile and León - Results of the Crop Survey with Accumulated data from the 2011-2018 Agricultural Campaigns"*. Instituto Tecnológico y Agrario de Castilla y León, Valladolid, Spain. https://www.inforiego.org/opencms/opencms/seguimiento_regadio/index.html - last accessed 22/01/2025.

Johnson, R.A., & Wichern, D.W. (2007). Applied Multivariate Statistical Analysis (6th ed.). Pearson Prentice Hall. ISBN 10: 0-13-187715-1.

Kostiakov, A. N. (1932). The dynamics of the coefficients of water percolation in soils and the necessity for studying it from a dynamic point of view for purpose of amelioration. Society of Soil Sci. 14: 17-21.

Kraijenhoff Van de Leur, D.A. (1958). A study of non-steady groundwater flow with special reference to a reservoir-coefficient. De Ingenieur (40), 87-94 (18) (PDF) Measuring and estimating water table level and drainage discharge rate in unsteady flow state. Available from: https://www.researchgate.net/publication/353480126_Measuring_and_estimating_water_table_level_and_drainage_discharge_rate_in_unsteady_flow_state - last accessed 22/01/2025.

Lewis, M. R. (1937). The rate of infiltration of water in irrigation practice. EOS Trans., American Geophysical Union 18: 361-368.

Lippera, M. C., Werban, U., & Vienken, T. (2023). Application of physical clogging models to Managed Aquifer Recharge: a review of modelling approaches from engineering fields. Acque Sotterranee - Italian Journal of Groundwater, 12(3), 9–20. https://doi.org/10.7343/as-2023-681 - last accessed 22/01/2025.

López Gunn, E., Rica, M., Zorrilla-Miras, P., Vay, L., Mayor, B., Pagano, A., Altamirano, M., Giordano, R. (2021). The natural assurance value of nature-based solutions: A layered institutional analysis of socio ecological systems for long term climate resilient transformation. Ecological Economics 186, 107053. https://doi.org/10.1016/j.ecolecon.2021.107053 - last accessed 22/01/2025.

Lopez-Gunn, E. (2021). Combining social network analysis and agent-based model for enabling nature-based solution implementation: The case of Medina del Campo (Spain). Science of the total environment 801, 149734. https://doi.org/10.1016/j.scitotenv.2021.149734 - last accessed 22/01/2025.

MAPA (1999). Proyecto de recarga del acuífero de la Cubeta de Santiuste de San Juan Bautista (Segovia) *"Project on the recharge of the Cubeta de Santiuste de San Juan Bautista aquifer (Segovia)"*. Secretaría General de Desarrollo Rural-Tragsatec. Unpublished technical report available for consultancy at MITECO´s library.

MAPA (2005). Asistencia técnica para el seguimiento y modelización de la recarga artificial en la cubeta de Santiuste de San Juan Bautista, Segovia *"Technical assistance for the monitoring and modelling of artificial recharge in the Santiuste de San Juan Bautista basin, Segovia"*. DGDR-TRAGSATEC (Unpublished Technical report available for consultancy in MAPA´s library).

MAPA (2009). Segunda asistencia técnica para el seguimiento y modelización de la recarga artificial en la cubeta de Santiuste de San Juan Bautista (Segovia). *"Second technical assistance for the monitoring and modelling of artificial recharge in the Santiuste de San Juan Bautista basin (Segovia)"*. Technical report available in MAPA´s library for public consultancy.

MIMAM (2002). Estudio del sistema de utilización conjunta de los recursos hídricos superficiales y subterráneos de las cuencas del Cega-Pirón y del Adaja- Eresma. *"Study of the system of conjunctive use of surface and groundwater resources in the Cega-Piron and Adaja-Eresma basins"*. MIMAM-PROINTEC.

MOPTMA (1994). Informe sobre la posibilidad de recarga artificial en la Cubeta de Santiuste (Segovia) *"Report on the possibility of artificial recharge in the Santiuste basin (Segovia, Spain)"*. Unpublished Technical report available for consultancy at MITECO´s library. Servicio Geológico de Obras Públicas, SGOP.

MAPAMA (2008). Gestión de la recarga de acuíferos: su implicación en la lucha contra la desertificación. Tipologías y dispositivos de recarga artificial *"Management of aquifer recharge: its implication in the fight against desertification. Types and devices for artificial recharge"*. https://www.miteco.gob.es/es/biodiversidad/temas/desertificacion-restauracion/0904712280144db8_tcm30-152640.pdf

MARSOL (2016a). MARSOL: Demonstrating Managed Aquifer Recharge as a Solution to Water Scarcity and Drought - Appropriate MAR methodology and tested knowhow for the general rural development (No. D5.3). MARSOL, Madrid, Spain. https://dinamar.tragsa.es/file.axd?file=/PDFS/marsol_d5-3_mar-technology_20160731.pdf - last accessed 22/01/2025.

MARSOL Fernández-Escalante, A.E., Calero Gil, R., Villanueva Lago, M., San Sebastián Sauto, J. (2016b). Demonstrating Managed Aquifer Recharge as a Solution to Water Scarcity and Drought (MARSOL). Managed Aquifer Recharge to Combat Groundwater Overexploitation at the Los Arenales Site, Castilla y León, Spain (No. D5.4). MARSOL, Madrid, Spain. https://dinamar.tragsa.es/file.axd?file=/PDFS/marsol_d5-4_arenales-final.pdf - last accessed 22/01/2025.

MARSOLut (2021). MARSoluT Periodic report, period 01.02.2019-28.02.2021. 1.2.4 WP 4 Optimizing Design (responsible: Enrique Fernández Escalante, Tragsa).

MARSOLUT. Fernández Escalante, A.E; Henao Casas, J.D., Calero Gil, R., San Sebastián Sauto, J., Wefer-Roehl, A., Schüth, C., Ayuga, F., Behle, V.R. and Sapiano, M. (2023a). Report on improving water quality at active MAR sites in Spain. MARSoluT, Deliverable 4.3. https://dinamar.tragsa.es/file.axd?file=/PDFS/d4.3final.pdf - last accessed 22/01/2025.

MARSOLUT. Henao Casas, JD., Fernández Escalante, A.E., Ayuga, F., Standen, K., Costa, L., Monteiro, JP., Vlassopoulou, A., Kallioras, A., Caligaris, E., Rossetto, R., Rudnik, G., Kurtzman, D., Sapiano, M. and Wefer-Roehl, A. (2023b). Report on the performance of optimal MAR designs. MARSOLut, deliverable 4-4, 2023. https://dinamar.tragsa.es/file.axd?file=/PDFS/d4.4final.pdf - last accessed 22/01/2025.

Matsuo, S. & Akai, K. (1952). A Field Determination of Permeability. https://repository.kulib.kyoto-u.ac.jp/dspace/bitstream/2433/280266/1/mfeku_14_4_225.pdf - last accessed 22/01/2025.

McGill, R., Tukey, J.W., Larsen, W.A. (1978). "Variations of Box Plots". The American Statistician. 32 (1): 12–16. DOI: 10.2307/2683468. JSTOR 2683468

METER (2016). Hydros 21 integrator guide. https://library.metergroup.com/Integrator%20Guide/18281_HYDROS21(CTD)_GEN1.pdf - last accessed 22/01/2025.

MOPTMA (1993). Estudio de caracterización de la unidad hidrogeológica "Región de Los Arenales" (02.17). *"Characterisation study of the hydrogeological unit "Región de Los Arenales"*. Report 2884. Servicio Geológico. Dirección General de Obras Hidráulicas.

Neuman, S.P. (1975). Analysis of pumping test data from anisotropic unconfined aquifers considering delayed yield, Water Resources Research, vol. 11, no. 2, pp. 329-342.

PHD (2016). Douro River Water Basin Plan. Spanish Official Bulletin BOE 16 Tuesday 19th of January of 2016 Sec. I. Pages. 3371-3372.

Rodgers, J.L., & Nicewander, W.A. (1988). Thirteen ways to look at the correlation coefficient. The American Statistician, 42, 59-66. DOI: 10.1080/00031305.1988.10475524 - last accessed 22/01/2025.

Sanz Montero, M.E, Arroyo, X., Cabestrero, O., Calvo, J.P., Fernández-Escalante, A.E., Fidalgo, C., García-del-Cura, M.A., García-Avilés, J., González-Martín, J.A., Rodríguez-Aranda, J.P., Rovira, J.V. (2013). Procesos de sedimentación y biomineralización en la laguna alcalina de las Eras. Humedal Coca-Olmedo *"Sedimentation and biomineralisation processes in the alkaline lagoon of Las Eras (Coca-Olmedo Wetland)"*. Geogaceta 53. ISSN 0213-683X.

SDEC (2006). Tensiometer with "Bourdon" manometer SR 1000. Soils Studies. http://www.sdec-france.com - last accessed 22/01/2025.

SDEC (2008). Humidimetre de sol. soil moisture sensor HMS 9000. SDEC France - Z.I de la Gare -37 310- Reignac sur Indre (France). http://www.sdec-france.com - last accessed 22/01/2025.

Terzaghi, K. and Peck, RB. (1967). Technology & Engineering. 752 pages. Ed. John Wiley & Sons. New York.

Theis, C.V. (1935). The relation between the lowering of the piezometric surface and the rate and duration of discharge of a well using ground-water storage, Trans. Am. Geophys. Union, 16, 519–524, 1935.

Thiem, A. (1906). Bericht über die Vorarbeiten zur Erweiterung der Wasserversorgung der Stadt Leipzig, 23 p., Leipzig, Thiem & Söhne, 1906.

Tragsa (2008). Proyecto de obra de las estaciones DINA-MAR ZNS. (DINA-MAR ZNS stations construction site Project). Tragsa Group. https://dinamar.tragsa.es/post/Instalacion-de-las-estaciones-Dina-Mar-de-Santiuste-y-Coca-(Segovia) - last accessed 22/01/2025.

Tragsa (2015). MARSOL 5-1 Deliverable. Los Arenales demonstration site characterisation. Report on the Los Arenales pilot site improvements (Restricted deliverable).

WEB SITES
Meteo data:
Inforiego. Station SG02, Nava de la Asunción. https://www.inforiego.org/opencms/opencms/info_meteo/index.html - last accessed 22/01/2025.
General information:
IAH. Commission on Managing Aquifer Recharge. International Association of Hydrogeologists. https://recharge.iah.org - last accessed 22/01/2025.
MARSOLUT project web site. www.marsolut-itn.eu - last accessed 22/01/2025.
DINAMAR. www.dinamar.tragsa.es - last accessed 22/01/2025.